Київ 2020

MINISRY OF EDUCATION AND SCIENCE OF UKRAINE

NATIONAL AVIATION UNIVERSITY

Departament of aircraft design

APPROVED BY
Head of department
Dr.Sc., professor.
_____S.R. Ignatovych
«_____» _____ 2020

MASTER THESIS
(EXPLANATORY NOTE)

EDUCATIONAL DEGREE
"MASTER"

THE EDUCATIONAL PROFESSIONAL PROGRAM
«AIRCRAFT EQUIPMENT»

Theme: «Optimization of the XZ latch design for Unit Load Devices»

Prepared by: _____ **A.S. Dakhovnik**

Supervisor: Dr.Sc., professor _____ **M.V. Karuskevych**

Consultants on separate chapters of the explanatory note:

labor protection:
PhD, associate professor _____ **O.V. Konovalova**

environmental protection:
PhD, associate professor _____ **L.I. Pavliukh**

Standard controller: _____ **S.V. Khizhnyak**

Kyiv 2020

NATIONAL AVIATION UNIVERSITY

Aerospace Faculty
Department of aircraft design
Educational degree «Master»
Specialty 134 «Aviation and space rocket technology»
Educational professional program «Aircraft equipment»

APPROVED BY
Head of department
Dr.Sc., professor.
_____S.R. Ignatovych
«_____» _____ 2020

TASK
for the master thesis

ANASTASIIA DAKHOVNIK

1. Theme: « Optimization of the XZ latch design for Unit Load Devices », approved by Rector's order № 1906/ст from October 5, 2020.
2. Period of work execution: from October 5, 2020 to December 13, 2020.
3. Initial data: cruise speed V_{cr}= 600 km/h, flight range L = 1350 km, payload 10 tons.
4. Content (list of topics to be developed): analysis of problems and contemporary XZ latch designs, methods and procedures, preliminary aircraft design as an object for the new design implementation, designing of new XZ latch construction, analysis of harmful and dangerous production factors, calculations of carbon monoxide and nitrogen oxide emission by aircraft.
5. Required materials: general view of the airplane (A1×1); layout of the airplane (A1×1); layout of roller equipment (A1×1); general view of ULD loading (A1×1); XZ latch placard (A1×1); roller section assembly (A1×1).
Graphical materials are performed in AutoCad, NX.

6. Thesis schedule

Task	Execution period	Signature
Task receiving, processing of statistical data.	5.10.2020– 12.10.2020	
Methods and procedures.	13.10.2020 – 16.10.2020	
Preliminary aircraft design.	17.10.2020 –19.10.2020	
Graphical design of the XZ latch.	20.10.2020 – 26.10.2020	
Strength calculation of the XZ latch.	27.10.2020 – 2.11.2020	
Static test of the XZ latch.	3.11.2020 – 9.11.2020	
Labor protection .	10.11.2020 – 14.11.2020	
Environmental protection.	15.11.2020 – 29.11.2020	
Complection of the explanation note.	30.11.2020 – 5.12.2020	

7. Special chapters consultants

Chapter	Consultant	Data, signature	
		Task issued	Task received
Labor protection	PhD, associate professor O.V. Konovalova		
Environmental protection	PhD, associate professor L.I. Pavliukh		

8. Date of issue of the task: «__»_____2020

Thesis supervisor _____ M.V. Karuskevych

The task was accepted for execution: _____ A.S. Dakhovnik

ABSTRACT

Master degree thesis «Optimization of the XZ latch design for Unit Load Devices»:

85 sheets, 38 figures, 9 tables and 16 references.

Object of study - the research and development process for the XZ latch for Unit Load Devices optimization.

Subject of study new design of the XZ latch for Unit Load Devices.

Aim of thesis - is the optimization of the XZ latch design for Unit Load Devices.

Research methods - comparative design analysis, stress-strain Finite Elements Analysis, static test of the latch assembly.

Novelty of the results - novelty of the design ensures improved reliability.

Practical value - acceleration of loading and unloading of ULDs, reducing of the aircraft downtime.

AIRCRAFT, PRELIMININARY DESIGN, ROLLER EQUIPMENT, XZ LATCH.

CONTENT

ABBREVIATIONS

ULD – Unit Load Device;

CLS – Cargo Loading System;

PDU – Power Drive Unit;

CAD – Computer Aided Engineering;

CAE – Computer Aided Engineering;

CAM – Computer Aided Manufacturing;

MAC - Mean Aerodynamic Chord;

CNC - Computer Numerical Control;

CG – Center of Gravity.

INTRODUCTION

The containers compartments of the contemporary aircraft are equipped with variety of the machanisms to unsure safety of loads, facilitating of the loading and unloadins processes, etc. Among mentioned equipment, the locks for the fastening containers deserve special attention due to the high requirements to their strength, simplicity and reliability of the work.

The aim of master thesis is designing of the improved XZ latch for factening ULDs and pallets on the roller tracks.

The objectives of the work are:

- State of the art literature analysis;
- Methods and procedures description;
- Calculation of plane geometry for research and development results implementation;
- Estimation of centering range;
- Presentation of new XZ latch construction;
- Determination of equivalent stresses occurring in construction in different loading variants;
- Analysis of harmful production factors;
- Aircraft emissions calculation;
- Development of recommendation for practical application of the result.

According to the task for the master thesis optimization of the XZ latch design for Unit Load Devices has been performed. Maximum equivalent stresses occurring in the capture part during landing and is equal 17938 kgf/cm^2.

The calculation of the XZ latch is established on the bases of the conceptual design proposed by Antonov Design Buero, but first time adopted for the plane in the presented work parameters.

Diploma work comprises also the parts devoted to the problems of Environmental and Labor protection.

The part “Environmental protection” considers pollution of the atmosphere from the aircraft engines.

The part “Labor protection” deals with CNC miller workplace and its dangerous production factor.

The drawing performed on the base of NX software. The stress-strain analysis has been conducted by Finite Elements Method in NX Nastran software application.

The preliminary design of the aircraft as well as new latch design have been carried out with account of the requirements for aircraft of transport category. Aircraft geometry and masses of components have been found according to the procedure developed at the Aircraft Design Department of National Aviation University.

The experience and conceptual designs of the Antonov Design Buero is used after critical analysis.

1 LATCHES FOR UNIT LOAD DEVICES. STATE OF THE ART

1.1 FEATURES OF CARGO TRANSPORTATION

A typical load loading system consists of the necessary equipment to move, guide and restrain the cargo. Power drives (PDUs) can be installed for semi-automatic movement of the ULD (Figure 1.1). These elements can be attached either directly or via pallets and floor fittings to the seat rails and floor structure. The choice of system depends to some extent on how well the ULDs layout with the necessary restraints matches the floor structure and seat rails [1].

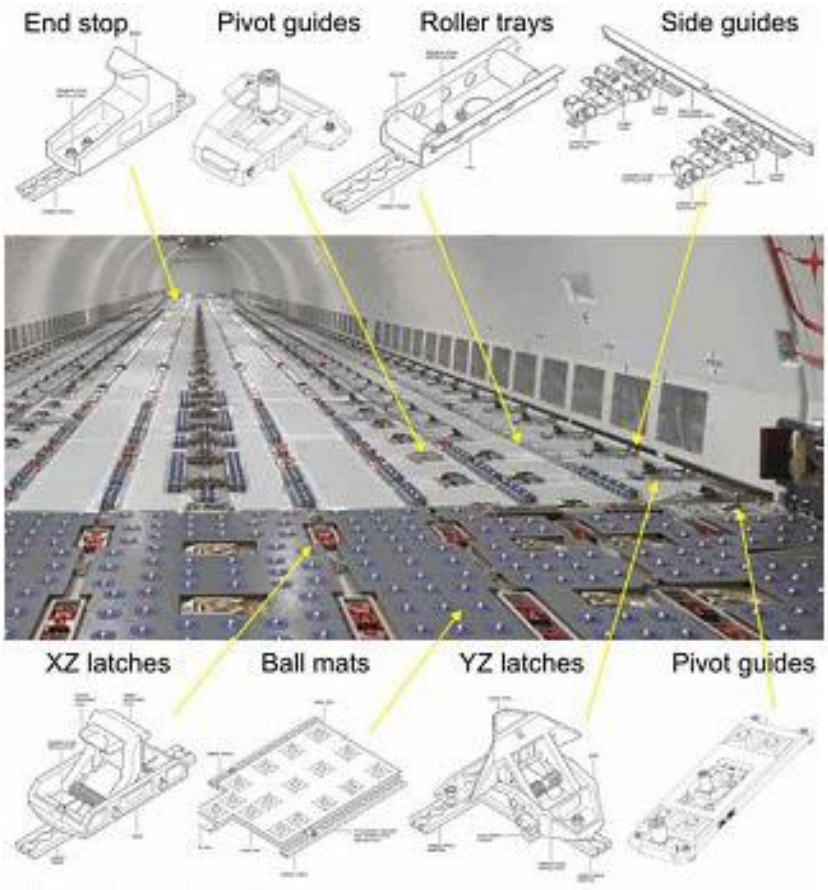

Figure 1.1 - Cargo loading system (CLS)

Tray assemblies provide flexible retention for various CLS parts such as locks and rollers (Figure 1.2).

The rollers allow free movement of ULD on the rails in both directions. Brake rollers restrict ULDs movement in one direction. They prevent the ULD from

unintentionally moving in sloped cargo compartments, especially towards the doorway.

Pallet locks hold pallets and containers. The longitudinal/vertical locking mechanism can be retracted below the plane of the roller to allow loading and unloading. The locks on the trays can be moved along the rails and secured to them with shear pins. End stop assemblies provide longitudinal and vertical restraint for pallets and containers at the beginning and end of the ULD row. They can be extended to facilitate unloading.

Hanging rails can be installed throughout the aircraft on either side of the door to protect the fuselage from damage and can include side locks. Side locks are used for vertical and lateral fixation. They are mounted either directly or via fittings onto an existing structure. Centerline guide nodes are installed along the centerline of the aircraft. They guide and hold ULDs that are loaded side-by-side along the centerline [2].

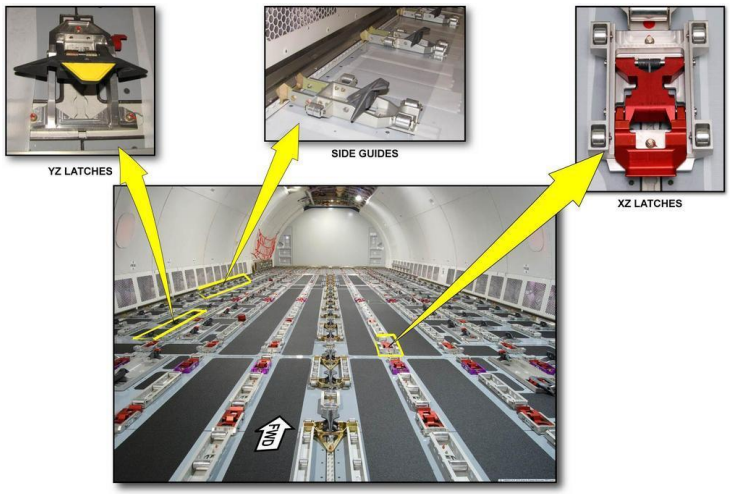

Figure 1.2 - ULD restraint system

Sill protection assemblies are installed when the cargo door is opened. They are attached to the seat rails with tension pins and positioned with shear pistons.

These items can be hinged so that they can be folded up when not in use. Roller and caster assemblies are mounted on sill guards to provide friction-reduced container movement. The hinged side guide is mounted on the outer edge of the sill. The side guide rises during use to guide containers through the cargo door.

To operate the aircraft safely, all hold cargo and baggage must be weighed must be properly loaded and secured to prevent movement in flight.

Loading must be carried out in full compliance with generally applicable rules and regulations, operator loading procedures and in accordance with the instructions of the person with overall responsibility for the loading process for the particular voyage. These loading instructions must comply with the baggage/cargo allocation requirements specified on the aircraft's cargo and trimming sheet [3].

1.2 Examples of compartment arrangements

The A350-900 (Figure 1.3) has three compartments, namely front, rear and cargo compartments and can load up to 36 LD3 containers or 11 standard 96 inches pallets. Special equipment is available for the transport of live animals, perishable goods, heavy pallets and vehicles.

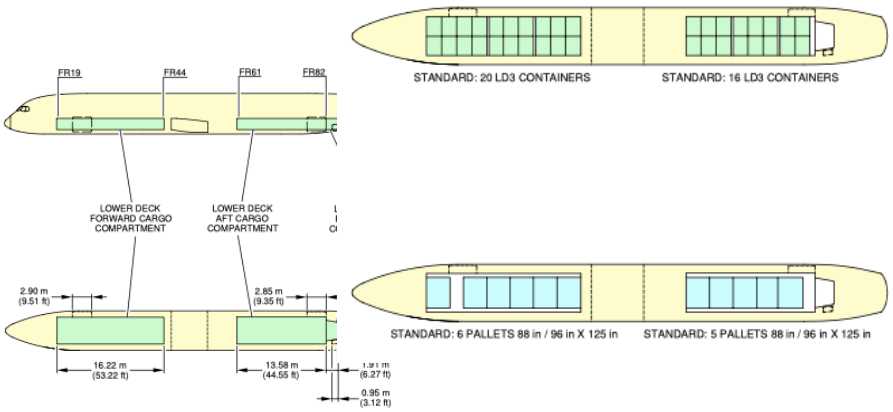

Figure 1.3 - A350-900 cargo compartment

To minimize aircraft turnaround time, the A350 XWB offers a high level of cargo hold capability and flexibility; 2 wide cargo doors and a Cargo Loading System (CLS), compatible with most lower deck cargo containers and pallet standards, allowing for stacking operations, simplify loading (Figure 1.4).

Figure 1.4 - A350-900 restraint system

The following figure compares the capabilities of the C-17, A-400, and C-130 (Figure 1.5).

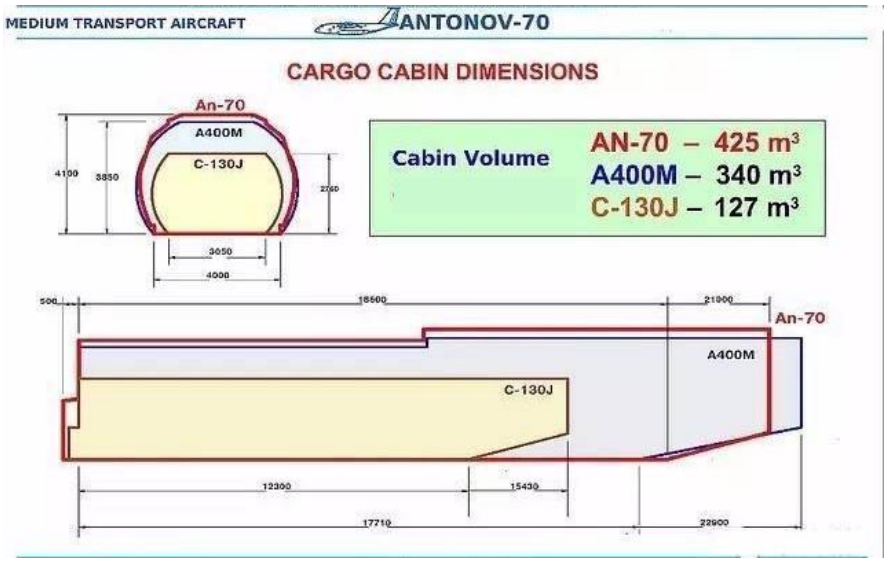

Figure 1.5 - An-70 is compared with A400M and C-130J

Cargo spaces compared to C-17, A400M and C-130-30 (Figure 1.6).

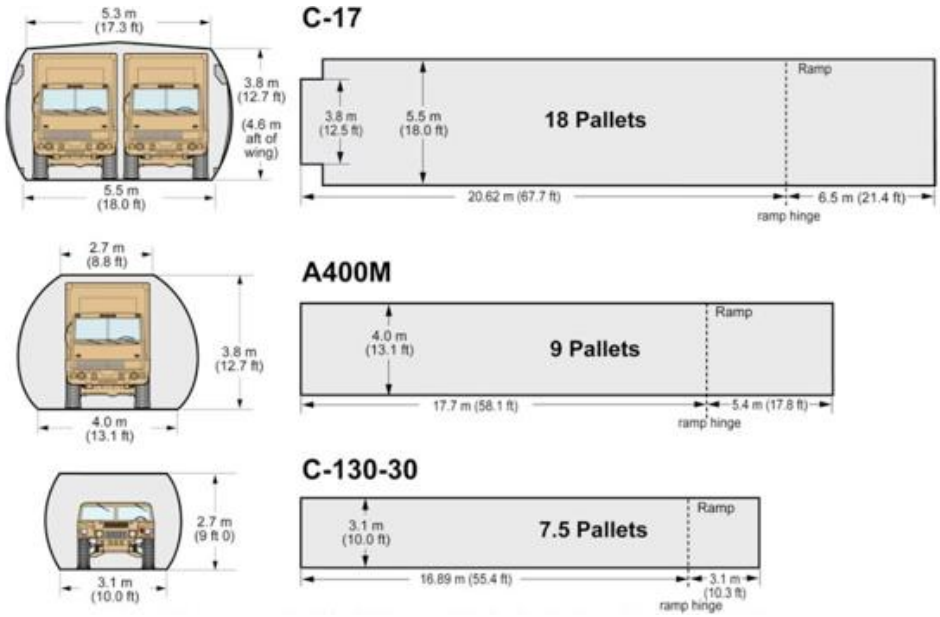

Figure 1.6 - Comparison of C-17, A400M and C-130-30

The cargo inside An-178 is shown in the Figure 1.7.

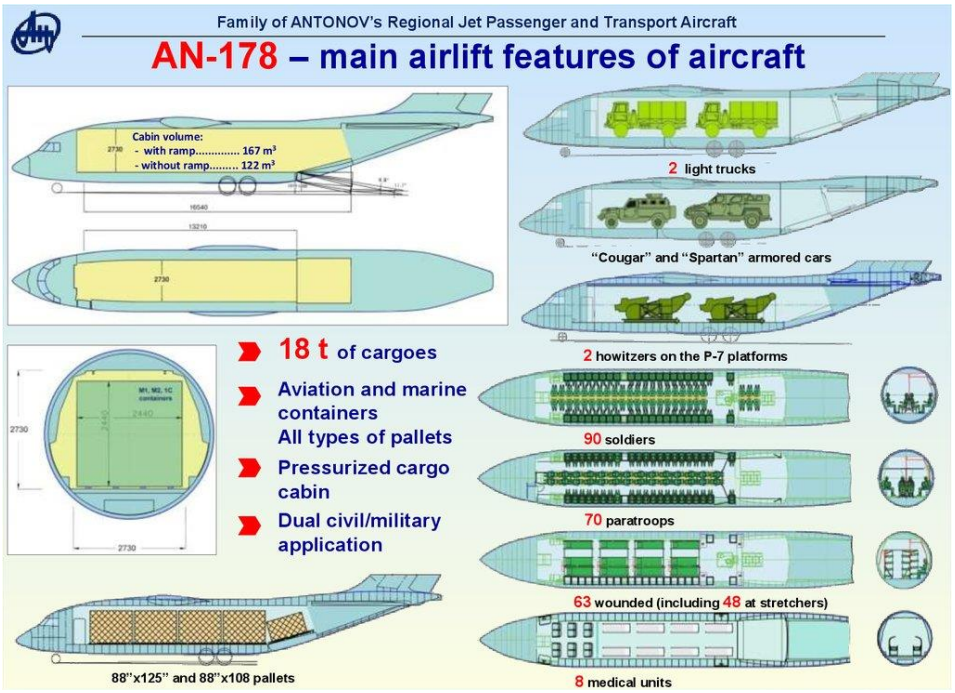

Figure 1.7 - An-178 cargo space

1.3 Detailed analysis of the contemporary designs

Two works directly related to the design of the XZ latch have been analysed.

1.3.1 Analysis of the contemporary advanced designs

Latch has been developed of the manufacturer of cargo handling and restraint systems ANCRA International, LLC [4]. Let's analyze the purpose, components and operation method of this lock.

The main purpose of this lock is to provide an automatic load securing device that can be installed on the floor of a commercial vehicle and which will remain in the retracted position until pallets are placed on the device in such a way as to trigger its automatic actuation.

In addition, the purpose of this lock is to provide a load securing device that is capable of automatically allowing unloading of pallets without the need for manual control.

Briefly, this is achieved by providing a pallet sensing mechanism so that the pallet can completely pass over and off the device without activating the locking mechanism. However, when the pallet comes to rest from its rear to the sensing mechanism, this causes the latching mechanism to become cocked, so the next pallet to arrive triggers the locking mechanism, that erects by locking the handles to secure the pallets in position. Means are also provided for automatic unloading such that removal of the second arriving pallet causes the locking arms to return to their retracted positions, allowing the first arriving pallet to be removed. Using this lock, it can be loaded and unloaded trucks without the need to manually lock pallets in place and without the risk of personal injury.

Referring to figures. 1.8-1.9, the front locking arm 1l and the rear locking arm 12 are shown in the raised position. The lock levers are pivotally supported by their root ends between the support plates 14 and 16 on the shaft or pivot pin 21. The lock levers and pivot pin may be made of a corrosion resistant material such as stainless steel. On either side of the locking levers, and also pivotally on the pin 21, there are sensor strips 22 and 24 formed from suitable high strength sheeting and having upwardly protruding fingers 37 formed at their front ends.

An H-shaped roller support bracket 26 is also attached to the pin 21, the lower levers of which are rotatably mounted at the ends of the pin 21 so as to encompass the sensor rods and the locking levers. At the other end of the roller support bracket, the shaft or roller pin 28 extends between the two arms of the bracket and extends through the entire thickness of the arms so as to extend beyond the outer surface of the arms on both

sides. The roller 30 is pressed onto the roller pin 28 and passes between the inner surfaces of the support roller by the arm of the weapon.

The roller support arm 26, the roller pin 28 and the roller 30, which will generally be referred to as the roller assembly 31, are free to pivot around the pivot pin 21. The downward movement of the roller assembly 31 is limited by the damper shaft or pin 35, which is parallel to the pivot pin 21 and the roller pin 28 and extends through the thickness of the base plates 14 and 16 so as to extend beyond their outer surfaces. Spring pins 39 are provided on both sides of the support plates to prevent lateral movement of the damper pin 35. The downward movement of the roller assembly 31 is also limited by arcuate grooves 41 recessed into the inner surfaces of the support plates 14 and 16, into which the ends of the roller pin 28 fit when the roller assembly is pressed downward.

Mounted on the shaft 35 is torsional resilient means or springs 38 having one end in contact with the lower surface of the locking lever forward 11 and the other end in contact with the lower surface of the cross member 27 of the support roller of the bracket 26. Spring 38 provides upward bias for assembly 31 roller, the upward movement of which is limited by pins 29, which protrude from the inner surfaces of the support plates 14 and 16.

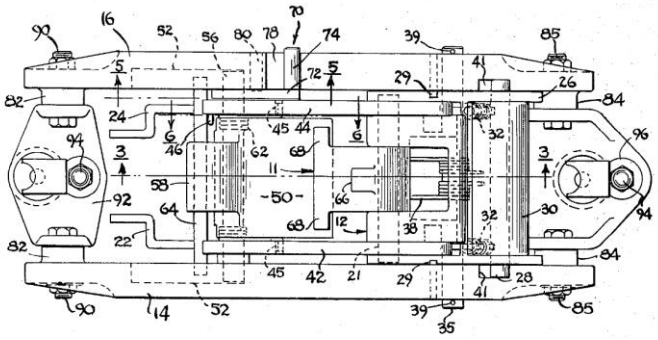

Figure 1.8 - A top view of a preferred embodiment of the pallet locking device according to the invention

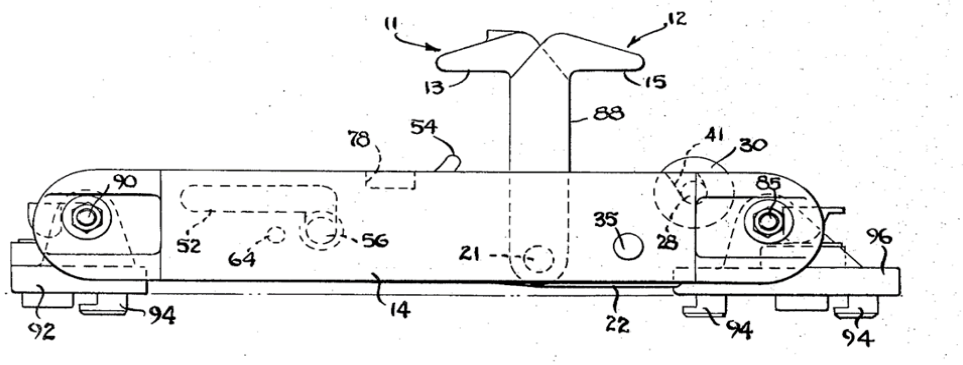

Figure 1.9 - A side view of the preferred embodiment of the invention in the locked position

In describing the automatic locking operation according to the present invention, reference is made to Figure 1.10, a-c), which shows the first cargo pallet 99 sliding into place. Only one of the sensor strips (i.e. 24) and associated connections are shown for convenience of illustration, and the other sensor strip 22 operates in synchronization with it. The locking levers 11 and 12 and the actuator arm assembly 50 are in the normal or retracted position with none of their parts protruding from the top surface of the support plates 14 and 16. For convenience of illustration, the locking levers and their connections are not shown in these figures. The pallet 99 slides unhindered on the upper surface of the device until it reaches the roller 30, whereupon, as shown in Figure 1.10, b), the weight of the pallet causes the roller assembly 31 to move downward, thereby compressing the springs 32, which in turn push the rear ends 36 of the strips 22 and 24 of the sensors down.

Since the sensor rods are pivotally mounted on the hinge pin 21, the front ends of the sensor rods with fingers 37 formed thereon move upward in response to the downward movement of the rear end 36. As shown in Figure 1.10, b), fingers 37 come into contact with the lower surface of the actuator arm 54, causing the actuator assembly 50 to rotate clockwise against the bias of the spring. The drive arm 54 rotates upward until it contacts the bottom surface of the pallet 99, whereupon it is kept from further rotation, thereby preventing the springs 32 from fully opening.

When the pallet 99 has slipped past the point at which it continues to hold the drive arm 54 from further rotation, as shown in Figure 1.10, c), the actuator arm pivots to a substantially vertical position in response to the force transmitted to it by fingers 37 springs 32, which continue to press downwardly on the rear end 36 of the sensor strips. If pallet 99 is not intended to be fixed in the position, it can be pushed further back in the vehicle, thereby reducing the downward force applied to the roller 30 and allowing the roller to return to the position shown in fig. 1.10. in response to the compression created by the springs 32, and the rotational displacement created by the spring. Thus, the rear end 36 of the sensor rods 22 and 24 can move upwardly to the position shown in Figure 1.10,

a), thereby weakening the force applied by the fingers 37 to the drive lever 54, after which the drive unit 50 returns to rotation. to its original position in response to the torque generated by the spring. The device is now completely retracted and any number of pallets can be passed through the device in this way without activating the locking mechanism. When the pallet 99 has reached the position where it is to be locked, it can stop on the roller assembly 31, thereby holding the device in the cocked position.

Referring now to Figure 1.10, d), the second pallet 101 is shown loaded on board the vehicle. When the edge of the pallet 101 contacts the drive arm 54, the drive arm assembly 50 is pushed back and its shaft 56 slides in the slots 52. When the drive arm assembly 50 is moved rearward, the drive link links 42 and 44 are pivotally pivotable attached to it, push horizontally on the carts 18 of the rear locking lever 12, thereby forcing it to rotate clockwise to the installed or vertical position. At the aft end, the locking lever 12 starts to rotate from the retracted position, it engages the cars of the locking lever forward 11 and pulls the catch forward in the upright position.

When the actuator arm assembly 50 is pushed against the rear end of the L-shaped slot 52 and cannot move further longitudinally, the arm assembly 50 will continue to rotate clockwise in response to the pallet push against the torque generated by the spring 62. As the pallet moves forward 10 continues to move rearward, it will apply a downward force to the lever assembly 50 so that its shaft 56 will move downwardly into the vertical portion 53 of the L-slot 52, thereby allowing the pallet 101 to move along the lever 54, locking it in position. With the lever assembly 50 locked, the actuation levers 42 and 44 serve to hold the locking levers 11 and 12 in an upright position as shown in Figure 1.10, e). Thus, the pallets 99 and 101 cannot slide in the longitudinal direction and are kept from significant vertical movement by the locking or horizontally protruding protrusions 13 and 15 located at the top of the locking arms.

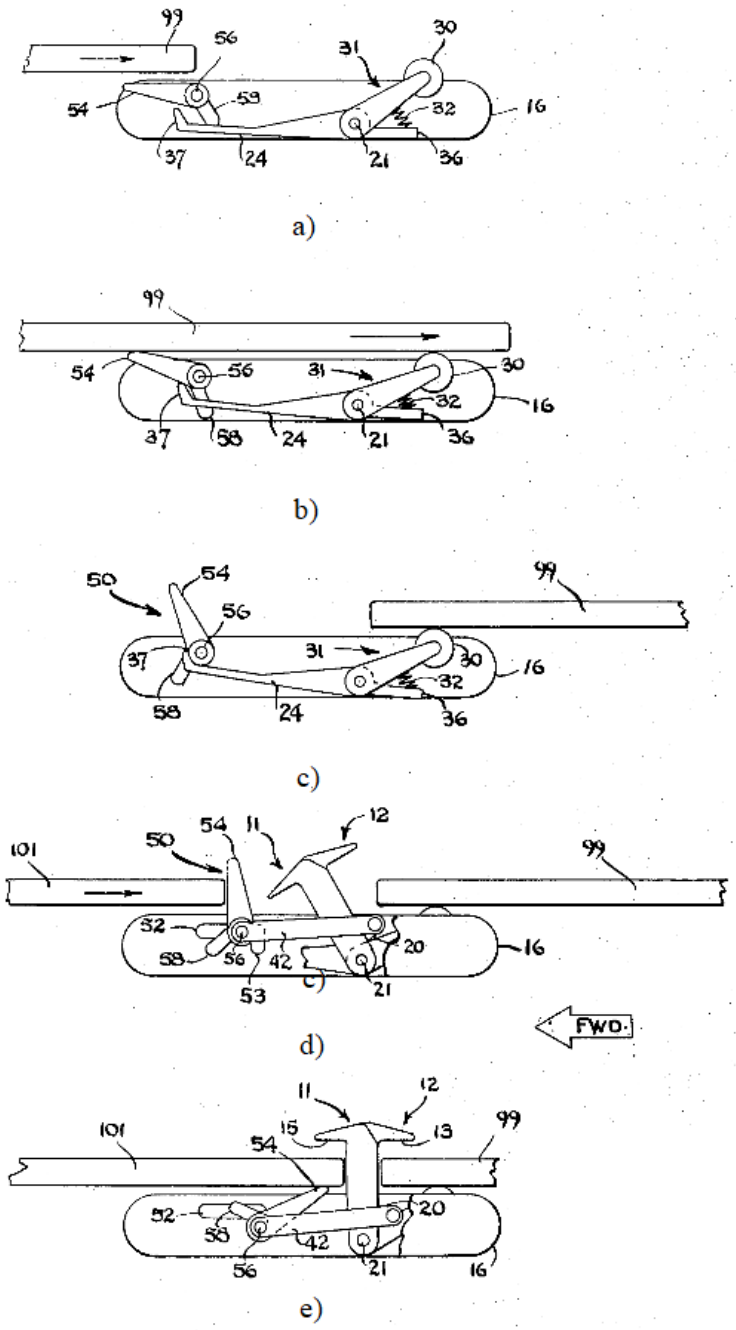

Figure 1.10 - A series of schematic views of the preferred embodiment of the invention sequentially illustrating the loading of pallets thereon

1.3.2 Basic principles of the new design

One more example was proposed early in the Bachelor's work special part and is considered now as a initial base for the improvement.

Figure 1.11 represents the locking device for securing freight containers to the freight deck of an aircraft. A plurality of locking hooks are pivotally secured to the flight

deck beneath the surface thereof. A resilient device is provided to urge the locking hooks to an upright position wherein the hook portion of the locking hook projects above the surface of the freight deck. The locking hooks, when in the retracted position beneath the surface of the freight deck are locked in position by a pin. Pin is a manually operated released.

The locking device consists of a housing-like frame, in the central area of which, locking hook 1 are pivotally supported about the axes 5 and 7.

As is shown in Figure1.11, the locking hook 1 has nose-like projections on it free ends, which projections engage in the swung-out or projecting condition corresponding recesses in the freight containers which are to be anchored.

The locking hook 1 is usually swung in against the spring force of a suitable spring so that the locking hook can stand up again in the swung-out position according to Figure 11 c) through the action of the stored energy in the spring.

To effect a release of the locking hook 1 so that it will move to the upright swung-out position, a so-called rocker 2 is used and which is pivotally supported about the pin 3 in the frame. The rocker 2 is constructed so it will be pivoted about the axis 4 and 7 in either direction, corresponding with the Figure 1.12 a) and b) cases.

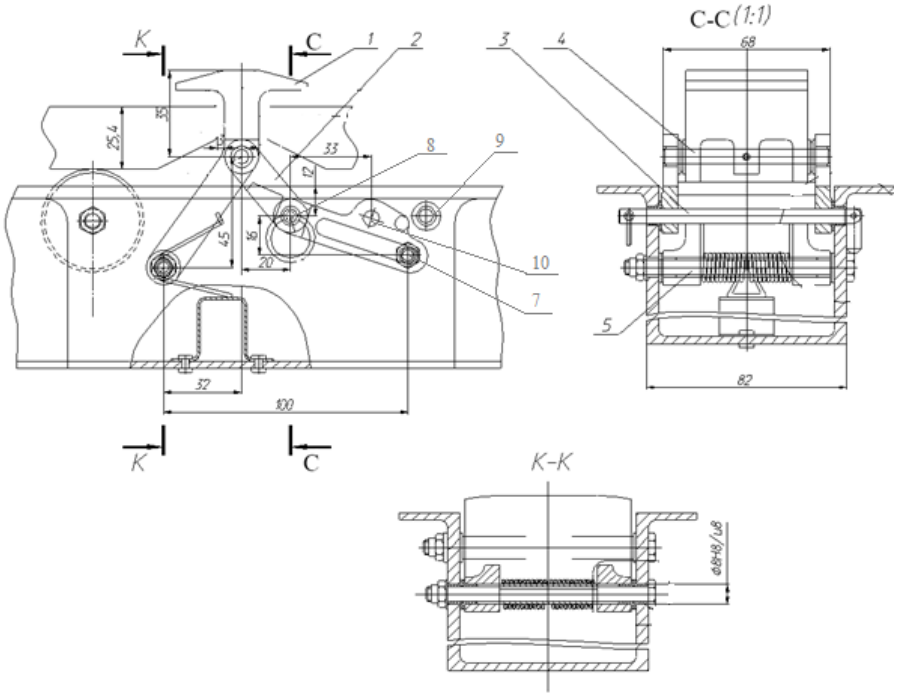

Figure 1.11 – Components of the XZ latch: 1 – Stop; 2 – Rocker; 3 – Pin; 4,5 – Axes; 5 – Screw; 6 – Sleeve

As is shown in Figure 1.12 to affect a retraction of the locking hook 1, pin 3 removes from the hole 8, than hook moves to the down position, in the same time hole 10 aligns with the hole 9. Finally, pin 3 sets in the hole 9.

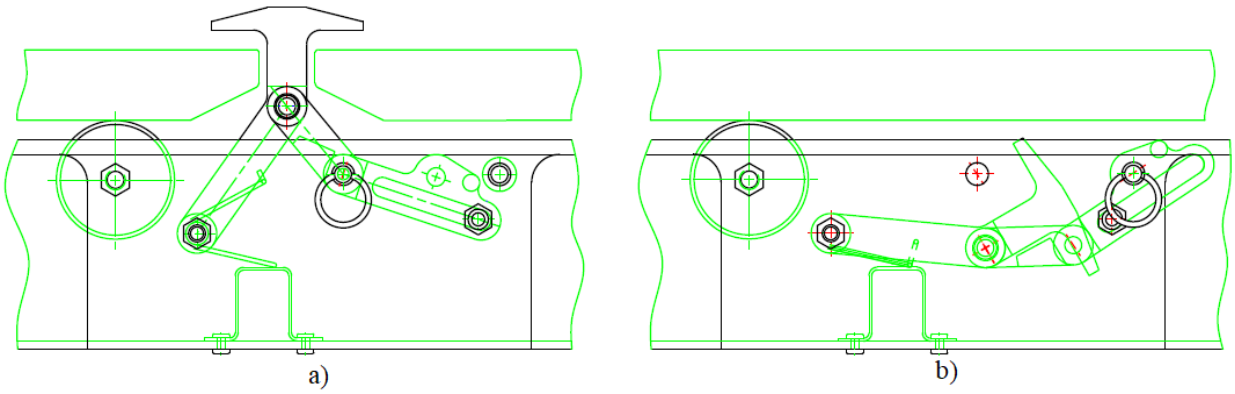

Figure 1.12 - XZ latch in: a) extended position; b) in retracted position

Conclusion to part 1

After getting acquainted with the options for fastening and accommodation of the cargo, it should be noticed that the restraint system has quite a lot of means of different desings and it is necessary to ensure the maximum reliability of these equipment.

After analyzing the contemporary advanced design, it was found some problems associated with his work. If we take a look at Figure 8- Figure 10, it can be seen that during loading and unloading of pallets or containers, their lower part is in contact with the actuator lever. With regular friction of the bottom of the pallet or container against the end of the actuator lever, the period of operation of these elements is reduced, and there is also the possibility of damage to one or another element.

Also, it was noticed that this lock consists of many elements, compared with locks with a similar application. In addition to the fact that such a sufficiently large number of elements makes this mechanism more expensive, the weight of the mechanism also increases, which also negatively affects the aircraft as a whole, as it affects flight performance and increases fuel consumption, which negatively affects both the economic component of companies, so on the environment.

Having reanalyzed the new design of the XZ latch, some shortcomings of this work were reaveled.

In this model of the lock, a pin was proposed as a fix mechanism, which now, is not relevant. In this design, to lock the stop in the retracted and extended position, you must manually fix the lock by manually installing the pin. During the loading or unloading of containers and pallets, it will take a lot of time to fix such lock, which in our time is not permissible for airlines due to the large number of flights, and this idle time for an aircraft will greatly affect the finances of airlines.

So, the aim of this work is the design opitimization of the lock fastening means mounting the cargo.

Main objectives of this paper are:

- to analyze fastening means for ULDs;
- to design XZ latch with:

- reduced number of elements in the mechanism;

- mechanism for retract and extand position with minimal time costs and effort for personal;

- the most profitable production.

- to develop preliminary design of the cargo aircraft for implementation of the designed XZ lath.

2 METHODS AND PROCEDURES

2.1. 3D modeling program

For 3D modeling of the XZ latch Siemens NX program was used. The 3D model of the capture is shown in Figure 2.1.

It is a 3-in-1 system, i.e. CAD+CAE+CAM. Offers a modern interface and advanced features, including:

support for a full cycle of product creation, from CAD (Modeling), then moving to CAE (Advanced Simulation) and ending with CAM;

an intuitive understandable interface for engineers who have experience in CAD-packages;

tools of synchronous modeling, allowing the most easy and quick to make changes to an existing or imported model;

the ability to create an "idealized" model, as well as a number of tools for preparing the model for calculation without affecting the base geometry;

extensive capabilities of the postprocessor at the stage of analysis and interpretation of simulation results, etc.

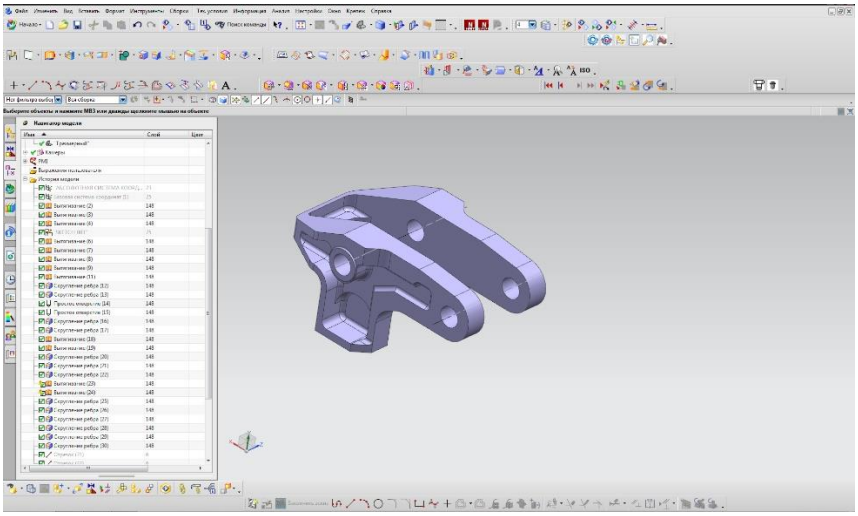

Figure 2.1 – 3D model created with Siemens NX program

Design (CAD). The set of applications included in the NX CAD package allows you to solve the problems of developing a complete electronic layout of the entire product and

its components for subsequent use in the processes of technological preparation of production.

The functionality of the applications allows to automazation the stages of product design and release of design documentation in various forms of presentation. Both "bottom-up" and "top-down" design technologies are supported, with the ability to build end-to-end development processes from product requirements to the stage of data output for production.

Industrial Design. Industrial design tools in NX are designed to develop the appearance of a designed product and analyze its aesthetic and visual characteristics. This functionality allows you to automate the design development processes from digitizing or creating two-dimensional sketches to analyzing technological processes for manufacturing external appearance elements and designing the corresponding equipment [6].

Mechanical systems development. The NX CAD system allows to simulate parts and assemblies of a product, conduct intersection analysis and mass calculations, prepare 2D documentation - drawings or 3D documentation using PMI (dimensions and annotations are applied to the 3D model). Using the toolkit of applications for modeling parts and assembly units, the user can create a complete digital analogue of the developed assembly or a single part, containing the exact geometry, calculated mass-inertial characteristics, material properties, as well as all the requirements necessary for manufacturing and control.

The capabilities of the system allow you to simulate products of any degree of complexity and dimension - from household appliances to products of the ship and aerospace industries. Electronic models created in NX CAD applications are used further in the modules of engineering analysis and technological preparation of production.

Engineering Analysis (CAE). The set of engineering analysis tools in the NX system is an application of pre- and post-processing and calculation solvers connected to the interface. Solvers can be either NX Nastran or third-party software packages. The engineering analysis environment can work both independently and in integration with the PLM system Teamcenter. In the latter case, all design data is stored in the PLM system and managed in terms of access rights, revisions, release and approval processes, etc [7].

The pre/post-processing application is built on the common NX CAD application platform and takes full advantage of the Parasolid geometry core. Calculation models are associated with the original 3D models, and if it is necessary to make any changes or simplifications, the user has the ability to edit the associative geometry without affecting the original model, but keeping track of all changes.

The functionality of the tools included in the NX engineering analysis package allows you to analyze the static loading of a structure, search for natural frequencies (dynamics), aerodynamic and thermal analysis, as well as solve a number of applied specialized problems.

2.2. Finite Element Method.

For Stress-Strain analysis of the XZ latch in the NX Nastran program Finite Element Method was applied.

A typical engineering task in FEM begins with the preparation of a model - a virtual analogue of a real building structure, technological product, mechanism part, etc.

Example of the FEA net is shown in Figure 2.2.

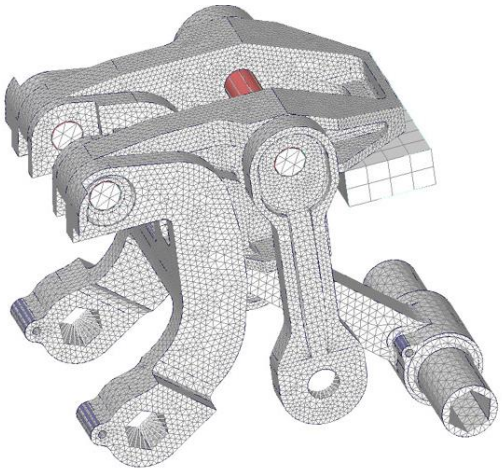

Figure 2.2 – Finite Elements computational model

From a geometric point of view, the computational model is a field of points connected to each other by primitives (straight line segments, triangles, rectangles, etc.). This is how a kind of mesh structure is formed - the geometry of the original structure is

approximated by the mesh superimposed on it, and further work is carried out not with the original system, but with the resulting mesh.

In addition to geometry, the primitives connecting the model nodes also have known mechanical properties. This means that by linking the stiffness of all mesh elements into a single whole (within the framework of the assumptions made in the model), it is possible to establish the stress-strain state of the entire system. So the calculator can get any factors of interest - longitudinal and transverse forces, bending and torsional moments, stresses, deformations, etc.

The number of nodes and elements that make up the design model is known in advance. For some complex systems, it can be measured in thousands or even millions, but it is, one way or another, of course. This circumstance, as well as the fact that the principle of "operation" of each individual element of the system is known in advance, gave rise to the name - the finite element method. And the mesh itself is called, as a rule, finite element.

From a mathematical point of view, the area in which the solution of the system of differential equations of the FEM is sought is divided into subdomains (elements), and for each element an approximating function of an arbitrary form is selected. The simplest and "rough" case is a polynomial of the first degree: outside the element, the selected function is equal to zero, and on the boundaries (at the nodes) the function takes values that are the solution to the problem. Of course, they are not known in advance. The coefficients of the polynomial of the approximating function are found from the conditions of equality of the values of neighboring functions at the nodes [8].

Next, a system of linear algebraic equations is compiled, in which the number of unknowns is equal to the number of degrees of freedom of the system (in the general case, this is six times the number of grid nodes). The dimensions of the grid are limited not only by a specific task, but also by the physical capabilities of the computer (primarily, by the size of available memory).

In the scientific and technical literature, the theory of the finite element method is presented through matrix calculus. The stages described above necessarily contain the collection of the stiffness and mass matrices of the structure. The stiffness matrix is a table

in which the nodal reactions of a finite element to an alternate single perturbation of each of its nodes are recorded. Simply put, the stiffness matrix of a finite element is a system of interconnections of all its points at the "mechanical" level. Knowing the local stiffness matrix of each individual element, a computer program (CAE) forms a global stiffness matrix, summing up the stiffness of all elements joined at common (adjacent) nodes, taking into account their orientation in space. As a result, a general system of relationships between all nodes of the design model is obtained.

Boundary conditions are subsequently imposed on the assembled matrices (that is, system anchors and supports are taken into account). The engineer also sets loads that simulate the effect of external forces on the structure, after which the resulting system of linear algebraic equations is solved by one method or another (for example, the Cholesky method is considered very effective). If the FEM is implemented in the form of a displacement method, then the result of the solution is the displacement of each structure node. The found nodal displacements can be used to find other factors of the stress-strain state.

FEM is a variational method. The energy functional for the entire area under consideration is here represented as the sum of functionals of its individual parts - finite elements. For the area of each element, independently of the others, its own distribution law of the sought functions is set. This piecewise continuous approximation is performed using specially selected approximating functions, also called coordinate or interpolating functions. With their help, the required continuous quantities (displacements, stresses, etc.) within each FE are expressed through the values of these quantities at the nodal points, and an arbitrary given load is replaced by a system of equivalent nodal forces.

With such a piecewise-continuous approximation, the compatibility condition is provided only at the nodes, and at the remaining points along the FE boundaries, this condition is satisfied approximately in the general case (in this connection, FE of different degrees of compatibility are distinguished).

In the design of machines, building structures, technological processes in scientific research, software complexes of computer engineering analysis (CAE) based on the finite element method (FEM) are widely used today. Examples of CAE complexes are the

software packages ANSYS, MSC.NASTRAN, MSC.MARC, COSMOS, ABAQUS, etc. They allow to numerically solve a wide variety of problems from such areas of physics as solid mechanics, fluid and gas mechanics, heat transfer, electrodynamics. Solution of related tasks is possible. There are specialized FEM-based packages that are designed for specific technical applications.

To effectively use these modern software tools, it is necessary to know not only the theory of the investigated physical process, but also to master the theory of FEM. It is also useful to have programming skills to understand the computer implementation of FEM.

The deformable body (structure) is divided into finite elements. The end elements can be of various shapes and sizes. As a result of splitting, a mesh is created from the boundaries of the elements. The intersections of these boundaries form nodes. Additional anchor points can be created on the borders and inside elements. An ensemble of all finite elements and nodes is the basis of the finite element model of a deformable body. The discrete model should cover the area of the object under study well enough.

2.3 Stress-Strain analysis program

For strength calculation of the XZ latch NX Nastran system was used. The fragment of the interface is presented in Figure 2.3.

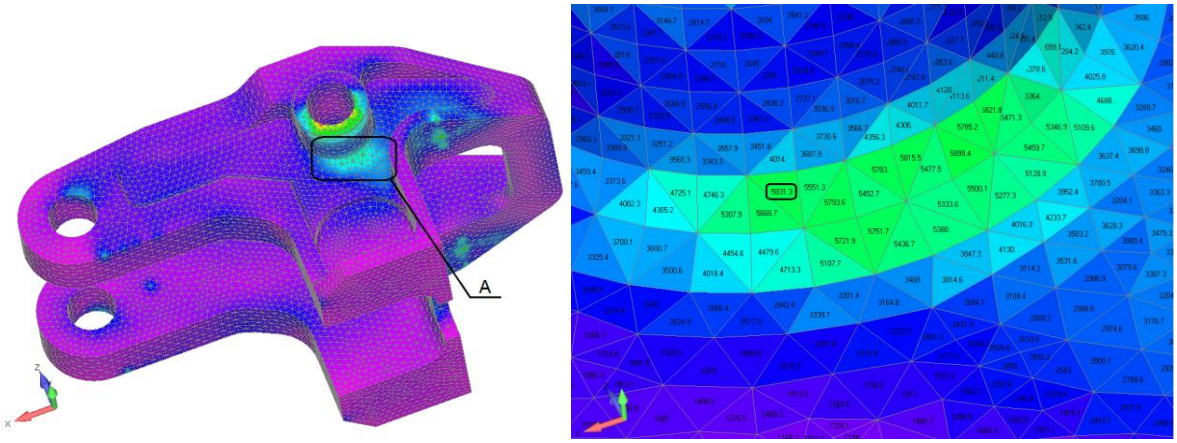

Figure 2.3 - Stress-Strain analysis: distribution of eqivalent stresses

NASA Structure Analysis. Developed by NASA and widely used in the aircraft and space industries. Nastran is open source, so the solver is used in many other CAE packages. Primarily focused on solving structural analysis problems.

Analysis models can be very large in size, requiring an extended period of time to solve. Such models can take hours or days to solve with traditional FEM applications. Nastran features a number of High-Performance Computing capabilities enabling engineers to solve large problems fast.

Assembly Modeling. Femap with NX Nastran allows modeling and analysis of assemblies, including an automatic detection tool for contacting bodies. Contact surfaces can be specified as direct contact (with / without friction) or glued together. The contact pairs involved in the calculation using NX Nastran are iteratively updated during the solution, taking into account the deformations that arise during the actual contact interaction.

Other technologies for modeling joints in assemblies are available: spot welding, fasteners and bolted connections with the ability to set preload.

Femap mesh generators, thanks to the extensive library of finite elements of the desired shape, allow to create high quality meshes and get accurate solution results. Femap gives full control over all mesh generation parameters such as mesh spacing, meshing for small details, ratios, consideration of small geometric elements, etc. With complex geometry, it is often necessary to modify the mesh in those areas where special calculation accuracy is required. Femap's Meshing Toolbox allows to do this simulation by interactively modifying the mesh spacing in the original model; the grid will update automatically. In addition, by modifying the mesh, using the graphical scale, can immediately analyze the quality of the created finite elements in order to make sure that the created finite element model meets the quality criteria [9].

Conclusion to part 2

After investigation the 3D modeling properties of the Siemens NX this program was chosen for the design of the new XZ latch.

For strength calculation of the restraint equipment supplemental program NX Nastran was used. Its calculation is based on Finite Element Method.

To create working conditions for the XZ latch, a preliminary aircraft design project was developed with the help of Discriminant analysis, so it was possible to classify data about different aircrafts features.

3 PRELIMINARY AIRCRAFT DESIGN AS AN OBJECT FOR RESEARCH RESULTS IMPLEMENTATION

Preliminary design has been performed for concretization of working conditions of the XZ latch.

3.1 Geometry calculations for the main parts of the aircraft

Knowing the predetermined basic parameters of the designed aircraft, as well as its geometric characteristics, it is possible to find the dimensions of the main parts of the aircraft: wing, tail, fuselage, engine nacelles, etc [11].

3.1.1 Wing geometry calculation

Wing area can be determined as:

$$S_w = \frac{m_0 g}{P} = \frac{41591 * 9.8}{3273} = 124{,}5\ (m^2), \tag{3.1}$$

where: m_0 -take-off weight.; P – specific wing load.

Wing span is:

$$l = \sqrt{S_w * \lambda} = \sqrt{124{,}5 * 10{,}34} = 35{,}9\ (m) \tag{3.2}$$

where: λ – wing aspect ratio.

Root chord is:

$$b_0 = 5{,}2\ (m) \tag{3.3}$$

Tip chord is:

$$b_t = 1{,}74\ (m) \tag{3.4}$$

The maximum wing width is determined by i-section of the forehead and span is equal to:

$$C_i = \bar{c} \times b_t = 0{,}11 \times 1{,}74 = 0{,}19\ (m) \tag{3.5}$$

On board chord for trapezoidal shaped wing is:

$$b_{ob} = b_0 \times \left(1 - \frac{(\eta_w - 1) \times D_f}{\eta_w \times l_w}\right) = 5{,}2 \times \left(1 - \frac{(3 - 1) \times 3{,}1}{3 \times 35{,}9}\right) = 4{,}9\ (m) \tag{3.6}$$

When choosing a wing power scheme, it is determined quantity of spars and their position, as well as the wing splitting points.

Calculative aircraft has three spars.

Relative position of the wing spars along the chord:

$$\bar{x}_i = \frac{x_i}{b} \tag{3.7}$$

In wing with two spars $\overline{x_1} = 0{,}2;\ \overline{x_2} = 0{,}6.$

Have been used the geometrical method for determining mean aerodynamic chord (Figure 3.1). Mean aerodynamic chord is equal: $b_{MAC} = 3.7\ (m)$

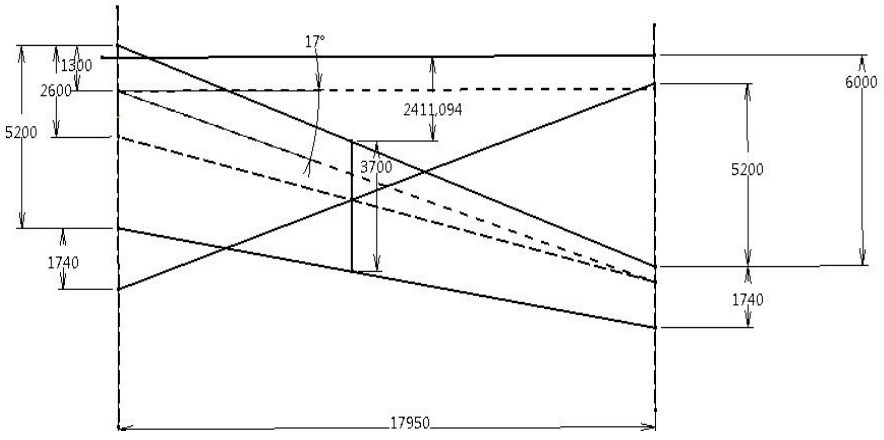

Figure 3.1. – Determination of mean aerodynamic chord

Geometrical parameters of the ailerons are determined as follows:

Ailerons span:

$$l_{ail} = 0{,}35 \times \frac{l_w}{2} = 0{,}35 \times \frac{35{,}9}{2} = 5{,}2\ (m) \tag{3.8}$$

Chord of aileron:

$$C_{ail} = 0{,}24 \times b_i = 0{,}24 \times 1{,}74 = 0{,}42\ (m) \tag{3.9}$$

Aileron area:

$$S_{ail} = 0{,}07 \times \frac{S_w}{2} = 0{,}07 \times \frac{124{,}5}{2} = 4{,}35\ (m) \tag{3.10}$$

Aerodynamic compensation of the aileron.

Axial:

$$S_{axinail} \leq (0.25 \ldots 0.28)\ S_{ail} = 0{,}26 \times 4{,}35 = 1{,}13\ (m^2) \tag{3.11}$$

Inner axial compensation

$$S_{inaxinail} = (0.3..0.31)\ S_{ail} = 0{,}3 \times 4{,}35 = 1{,}3\ (m^2) \tag{3.12}$$

For two engine airplane:

$$S_{tr.ail} = 0{,}05 \times S_{ail} = 0{,}05 \times 4{,}35 = 0{,}22\ (m^2) \tag{3.13}$$

Aileron deflection range

Upward $\delta'_{ail} \geq 5$;

Downward δ”$_{ail} \geq 15^{\circ}$.

The purpose of determining geometrical parameters of wing high-lift devices is to ensure the take-off and landing coefficients of wing lifting force, adopted in the previous calculations at the selected rate of high-lift devices and the type of the airfoil profile.

Before carrying out following calculations, it is necessary to select the type of airfoil from the airfoil catalog, indicate the value of lift coefficient $C_{y\max bw}$ and determine required increase for this coefficient $C_{y\max}$ for the high-lift devices outlet by the formula:

$$\Delta C_{y\max} = (\frac{C_{y\max l}}{C_{y\max bw}}) \tag{3.14}$$

Where $C_{y\max l}$ is necessary coefficient of lift in the landing configuration of the wing by the aircraft landing insuring (determined when choosing is the aircraft parameters).

In the modern design the rate of the relative chords of wing high-lift devices for three slotted flaps is:

$$b_f = 0.3..0.4\times b_i = 0.13 \times 1{,}62 = 0{,}21 \tag{3.15}$$

3.1.2 Fuselage layout

When choosing the shape and the dimensions of fuselage cross-section, aerodynamic and structural demands are considered.

As applied to the subsonic cargo aircrafts (V < 800 km/h) wave resistance doesn’t affect it. Therefore, needed to choose from the conditions of the list values friction resistance C_{xf} and profile resistance C_{xp}.

During the transonic and subsonic flights, shape of fuselage nose part affects the value of wave resistance C_{xw}. Application of circular shape of fuselage nose part significantly diminishing its wave resistance.

For transonic airplanes fuselage nose part has to be:

$$l_{npf} = 2 \times D_f = 2 \times 3{,}14 = 9{,}3 \tag{3.16}$$

In addition to aerodynamic requirements consideration when choosing a cross-section shape, we need to take into account strength and layout requirements [12].

To ensure minimum weight, the most convenient fuselage cross-section shape is circular cross-section. In this case the minimal fuselage skin width is get. As a partial case may be used the combination of two or more vertical or horizontal series of circles.

For cargo aircrafts the aerodynamics is not so important in the fuselage shape choice, and the cross-section shape is may be close to rectangular.

Geometrical parameters are concerned: fuselage diameter D_f; fuselage length l_f; fuselage fineness ratio λ_f; fuselage nose part fineness ratio λ_{np}; tail unit fineness ratio λ_{TU}. Fuselage length is determined considering the aircraft scheme, layout and airplane center of gravity position features, and the conditions of landing angle of attack α_{land} ensuring.

Fuselage length is equal:

$$l_f = \lambda_f \times D_f = 9 \times 3{,}14 = 28{,}21\ (m) \tag{3.17}$$

Fuselage nose part fineness ratio is equal:

$$\lambda_{fnp} = \frac{l_{fnp}}{D_f} = \frac{6{,}2}{3{,}1} = 2 \tag{3.18}$$

Sum of nose part and rear part fineness ratio:

$$\lambda_{fnp} + \lambda_{frp} = 5 \tag{3.19}$$

So, fineness ratio of rear part is equal:

$$\lambda_{frp} = 5 \; - \; \lambda_{fnp} = 3 \tag{3.20}$$

Length of the fuselage rear part is equal:

$$l_{frp} = \; \lambda_{frp} \times D_f = \; 3 \times 3{,}14 = 9{,}3 \tag{3.21}$$

3.1.3 Layout and calculation of basic parameters of tail unit

One of the most important tasks of the aerodynamic scheme is the choice of tail unit placement. To ensure longitudinal stability during overloads, its center of gravity should be placed in front of the aircraft focus and the distance between these points, related to the mean value of wing aerodynamic chord, determines the rate of longitudinal stability.

$$m_x^{Cy} = \bar{x}_T - \bar{x}_F < 0 \tag{3.22}$$

Where m^{Cy}_x –is the moment coefficient; $x_{T.}$ x_F- center of gravity and focus coordinates. If m^{Cy}_x=0, then the plane has the neutral longitudinal static stability, if m^{Cy}_x>0, then the plane is statically unstable. In the normal aircraft scheme (tail unit is behind the wing), focus of the combination wing – fuselage during the install of the tail unit of moved back.

Static range of static moment coefficient: horizontal A_{htu}, vertical A_{vtu} given in the table with typical arm Htu and Vtu correlations. Using table, may found the first approach of geometrical parameters.

Determination of the tail unit geometrical parameters.

Area of vertical tail unit is equal:

$$S_{VTU} = (0{,}18 \ldots 0{,}25) S_w = \; 29{,}02 \; (m^2) \tag{3.23}$$

Area o horizontal tail unit is equal:

$$S_{HTU} = (0{,}12 \dots 0{,}2)S_w = \ 29{,}02\ (m^2) \quad (3.24)$$

Values L_{htu} and L_{vtu} depend on several factors. First of all, their value are influenced by: the length of he nose part and tail part of the fuselage, sweptback and wing location, and also from the conditions of stability and control of the airplane.

Determination of the elevator area and direction:

Altitude elevator area:

$$S_{el} = (0{,}3 \dots 0{,}4)S_{HTU} = 0{,}35\ \times 29{,}02 = 10{,}1\ (m^2) \quad (3.25)$$

Choose the area of aerodynamic balance.

$$If\ ,0{,}6 \geq M \geq 0{,}3,\ \text{so}\ S_{eb} = (0{,}22 \dots 0{,}25)\ S_{el} \quad (3.26)$$

Elevator balance area is equal:

$$S_{el} = S_{EL} * 0{,}23 = 0{,}23 * 10{,}1 = 2{,}32\ (m^2) \quad (3.27)$$

The area of altitude elevator trim tab:

$$S_{te} = S_{EL} * 0{,}1 = 0{,}1 * 10{,}1 = 1{,}01\ (m^2) \quad (3.28)$$

Root chord of horizontal stabilizer is:

$$l_{HTU} = (0{,}31 \dots 0{,}5)l_w = 35{,}9 * 0{,}31 = 11{,}172\ (m) \quad (3.29)$$

$$b_{oHTU\ ROOT} = \frac{2S_{HTU} \times \eta_{HTU}}{(1 + \eta_{HTU}) \times l_{HTU}} = \frac{2 \times 29{,}02\ \times 2{,}5}{(1 + 2{,}5) \times 11{,}172} = 3{,}8\ (m) \quad (3.30)$$

Tip chord of horizontal stabilizer is:

$$b_{0HTU\ TIP} = \frac{b_{oHTU\ ROOT}}{\eta_{HTU}} = \frac{3{,}71}{2{,}5} = 1{,}5\ (m) \tag{3.31}$$

The geometry of vertical stabilizer is adjusted according to the design experience of this class aircraft.

Root chord of vertical stabilizer is:

$$b_{oHTU\ ROOT} = 5{,}1\ (m) \tag{3.32}$$

Tip chord of vertical stabilizer is:

$$b_{0VTU\ TIP} = 4\ (m) \tag{3.33}$$

3.1.4 Landing gear design

At the primary design stage, when the airplane center-of-gravity position is determined and there is no drawing of airplane general view, only the part of landing gear parameters may be determined.

Main wheel axel offset is:

$$e = b_{MAC} \times (0{,}15 \ldots 0{,}2) = 0{,}2 \times 3{,}72 = 0{,}75\ (m) \tag{3.34}$$

With a large axial wheel displacement, it is difficult to lift the front gear during take-off, and with small, the airplane may drop on the tail, when the loading of the rear of the aircraft comes first. Landing gear wheel base comes from the expression:

Landing gear wheel base comes from the expression:

$$B = (0{,}3 \dots 0{,}4)L_f = (6 \dots 10)e = 0{,}304 \times 28{,}21 = 8{,}6\ (m) \quad (3.35)$$

The last equation means that the nose support carries 6...10% of aircraft weight.

Front wheel axial offset will be equal:

$$d_{ng} = B - e = 3{,}75\ (m) \quad (3.36)$$

Wheel track is:

$$T = (0{,}5 \dots 1{,}2)B \leq 12\ m = 0{,}53 \times 8{,}6 = 4{,}6\ (\text{m}) \quad (3.37)$$

On a condition for avoiding of the side nose-over the value K should be > 2H, where H – is the distance from runway to the center of gravity.

Wheels for the landing gear is chosen according to the size and running load on it from the take-off weight; for the front support is considered dynamic loading also.

Type of the pneumatics (balloon, half balloon, arched) and the pressure in it is determined by the runway surface to be used. Breaks on the main wheel are installed.

The load on the wheel is determined:

K_g =2.0 – dynamics coefficient.

Nose wheel load is equal:

$$P_{NLG} = \frac{(9{,}81 \times e \times k_g \times m_0)}{(B \times z)} = \frac{(9{,}81 \times 0{,}75 \times 2 \times 41591)}{(16{,}46 \times 2)} = \frac{612011}{16{,}92} = 36170{,}86\ (N) \quad (3.38)$$

Main wheel load is equal:

$$P_{MLG} = \frac{(9{,}81 \times (B - e) \times m_0)}{(B \times z \times n)} = \frac{(9{,}81 \times (8{,}46 - 0{,}75) \times 41591)}{(8{,}46 \times 4)} \quad (3.39)$$

$$= \frac{3145739{,}4}{33{,}84} = 92959{,}2\ (N)$$

Table 3.1 - Aviation tires for designing aircraft

MLG		NLG	
Tire size	Tread design	Tire size	Tread design
24x8.0-13	Aircraft Rib	B46x16.0-21	Aircraft Rib

3.1.5 Cargo compartment design

Roller equipment is nowadays distributed in many areas and is a universal element of cargo transportation.

The roller section is one of the elements of the lower loading equipment of the aircraft, designed for moving and mooring pallets with cargo in the cargo compartment.The structure of the roller section № 4 includes a profile on which rollers are installed (9 pcs.), an XZ latch (1 pc.), two-mushroom units (4 pcs.) and a three-cork unit (1 pc.). The design of the roller section, roller, two-mushroon and three-cork assemblies is shown in Figure 3.2. The three-cork and two-mushoom assemblies are used to fix the roller section to the rail of the aircraft cargo floor. The rollers are designed to move pallets with cargo along the cargo compartment, and the XZ latch for mooring them. The design of the end lock is shown in Figure 3.3.

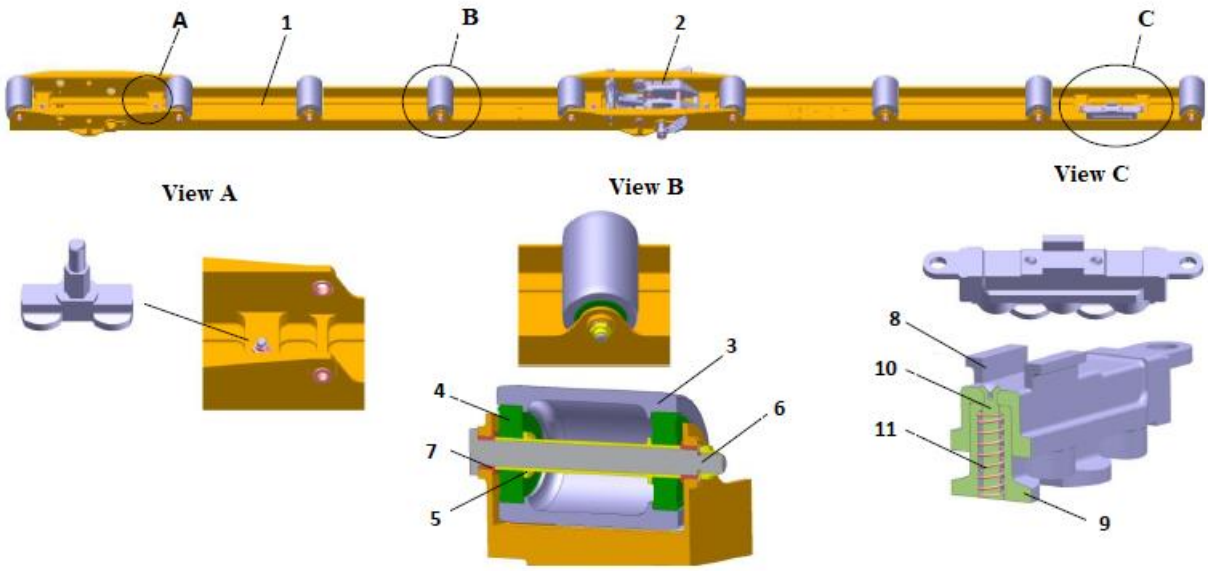

1. Profile
2. XZ latch
3. Clip
4. Bearing
5. Sleeve
6. Bolt
7. Sleeve
8. Retainer
9. Body
10. Axis
11. Spring

Figure 3.2 - The roller section, roller, two-mushroon and three-cork assemblies

3.1.6 Choice and description of power plant

Table 3.2 - Examples of application Д-36

Model	Thrust	Bypass ratio	Dry weight
ТРД Д-36	(65 kN)	5.6	1 124 kg

The engine compressor is axial, three-stage, consists of a single-stage supersonic fan, a near-sonic six-stage low-pressure compressor (LPC) and an up-to-sound seven-stage high-pressure compressor (HPC). LPC and HPC have air bypass valves.

3.2 Determination of the aircraft center of gravity position

3.2.1 Determination of centering of the equipped wing

Weight of the equipped wing includes the mass of its structure, mass of the equipment placed in the wing and mass of the fuel. Regardless of the place of attachment point (to the wing or to the fuselage), the main landing gear and the front gear are included

in the mass register of the equipped wing. The mass register includes names of the objects, mass themselves and their center of gravity coordinates. The origin of the given coordinates of the mass centers is chosen by the projection of the nose point of the mean aerodynamic chord (MAC) for the surface XOY. The positive meanings of the coordinates of the mass centers are accepted for the end part of the aircraft.

The example list of the mass objects for the aircraft, where the engines are located under the wing, included the names given in the table 3.3.

The example list of the mass objects for the aircraft, where the engines are located on the wing, included the names given in the table 3.3. The mass of AC is 91295 kg.

Power coordinates for the equipped wing are defined by the formulas.

N	Name	Mass		C.G. coordinates (m)	Moment (kgm)
		Units	total (kg)		
1	Wing (structure)	0,14	6057,72	1,61	9700,36
2	Fuel system,	0,01	170,52	1,61	273,06
3	Control system, 30%	0,01	101,06	2,23	225,82
4	Electrical equip. 10%	0,01	89,004	0,37	33,14
5	Anti-icing system 50%	0,01	357,68	0,37	133,21
6	Hydraulic system, 70%	0,02	608,47	2,23	1359,57
7	Power units	0,07	2952,96	-2,45	-7234,75
8	Equiped wing without below	0,24	10337,44	0,43	4490,41
9	Nose landing gear 15%	0,01	321,11	-6,53	-2099,37
10	Main landing gear 85%	0,04	1819,58	1,86	3388,06
11	Fuel	0,14	5889,28	1,48	8772,67
12	Equiped wing	0,44	18367,41	0,79	14551,79

Table 3.3 - Trim sheet of equipped wing masses

3.2.2 Determination of the centering of the equipped fuselage

Origin of the coordinates is selected in the projection of the fuselage nose on the horizontal axis. For the axis X the construction part of the fuselage is given. The list of the objects for the AC, which engines are mounted under the wing, is given in Table 3.4.

Table 3.4 - Trim sheet of equipped fuselage masses

1	2	3		4	5
№	Objects	Mass		Coordinates of C.G.(m)	Moment (kgm)
		Units	Total (kg)		
1	Fuselage	0,15	6528,53	14,1	92052,41
2	Horizontal tail unit	0,01	806,44	27	21774,14
3	Vertical tail unit	0,02	902,94	25,5	23024,98
5	Radar equipment	0,01	245,38	1	245,38
6	Instrument panel	0,0104	432,54	5	2162,73
7	Air-navigation system	0,01	370,15	3	1110,48
8	Radio equipment	0,01	187,15	3	561,47
9	Toilet 1	0,01	61,01	4,5	274,51
10	Rear cargo equipment	0,01	355	24	8520
11	Control system, 70%	0,01	235,82	14,1	3325,07
12	Electrical equipment, 90%	0,02	801,04	14,1	11294,71
13	Hydraulic system, 30%	0,01	260,77	19,747	5149,53
14	Air conditioning system equipment 30	0,01	214,61	14,1	3025,99
15	Decorative paneling	0,01	160,12	14,1	2257,76
16	Heat and sound isolation	0,0	320,25	14,1	4515,53
17	Water 1	0,0003	13,17	4,5	59,26
18	Anti-icing system, 20%	0,01	143,07	22,56	3228,87
19	Tools	0,01	432,54	4	1730,18
20	Pass. cabin add. equipment	0,001	41,59	19	790,22
21	Rescue equipment	0,0001	5,85	19	111,19
22	Seats of crew	0,001	60	3	180
23	Load Master	0,01	70	4	280

24	Auxiliary power unit	0,03	145,85	13	1896,17
29	Non-typical equipment	0,01	79,02	25	1975,57
	Total	0,55	23222,92	14,59	338886,19
25	Equiped fuselage without comercial loads	0,31	12793,91	14,66	187570,64
26	Crew	0,01	280	2	560
27	Cargo	0,24	9999,99	14,85	148499,97
28	Attendants 1	0,01	70	4	280

Ending of Table 3.4

3.2.3 Calculation of center of gravity positioning variants

The list of object masses for center of gravity variant calculation is given in Table 3.5 and center of gravity calculation options is given in table 3.6, completed on the basis of both previous tables.

Table 3.5 - Calculation of C.G. positioning variants

Name	Mass, kg	Coordinates	Moment
Object	m_i	C.G. (m)	kgm
Equiped wing without fuel and L.G.	10337,44	12,85	132911,71
Nose landing gear (retracted)	321,11	2	642,21
Main landing gear (retracted)	1819,58	11,40	20743,27
Fuel	5889,28	14,48	85333,39
Equiped fuselage	12793,91	14,66	187570,64
Cargo	10 000	14,6	146000
Crew	280	2	560
Attendants 1	70	4	280
Nose landing gear (opened)	321,11	3	963,31
Main landing gear (opened)	1819,58	11,4	20743,27

Table 3.6 - Airplanes C.G. position variants

п	Name of objects	Mass, kg	Mo men, kgm	C.G. m	ering

1	Take-off mass (L.G.retrackted)	41511,31	574041,23	13,82	26,0
2	Take-off mass (L.G. openedd)	41511,31	574362,33	13,83	26,2
3	Landing variant (L.G. opened)	40711,14	562447,09	13,81	25,7
4	Transportation variant (without payload)	31511,31	428362,33	13,59	19,7

Ending of Table 3.6

5	Parking variant (without fuel and payload)	25272,03	342188,94	13,54	18,3

Conclusion to part 3

Preliminary design has been performed for the structural integration of the new equipment and aircraft.

Designed plane meets current airworthiness requirement and trends in aviation industry.

The possibility to carry pallets of NAS 3610 standard with dimensions of 88x125 inches is presumed.

4 RESEARCH AND DEVELOPMENT RESULTS AND DISCUSSION

Equipment installed on the floor of an aircraft cargo compartment is intended to restrain aircraft unit load devices against the ground/flight loads. The XZ-latches are used to lock the ULDs in X- and Z-direction. Depending on the cargo hold configuration single or double may be installed to accommodate any kind of ULD loading. In this Part static testing and the strength calculation of the new designed XZ latch are presented.

4.1 Optimized design of the XZ latch

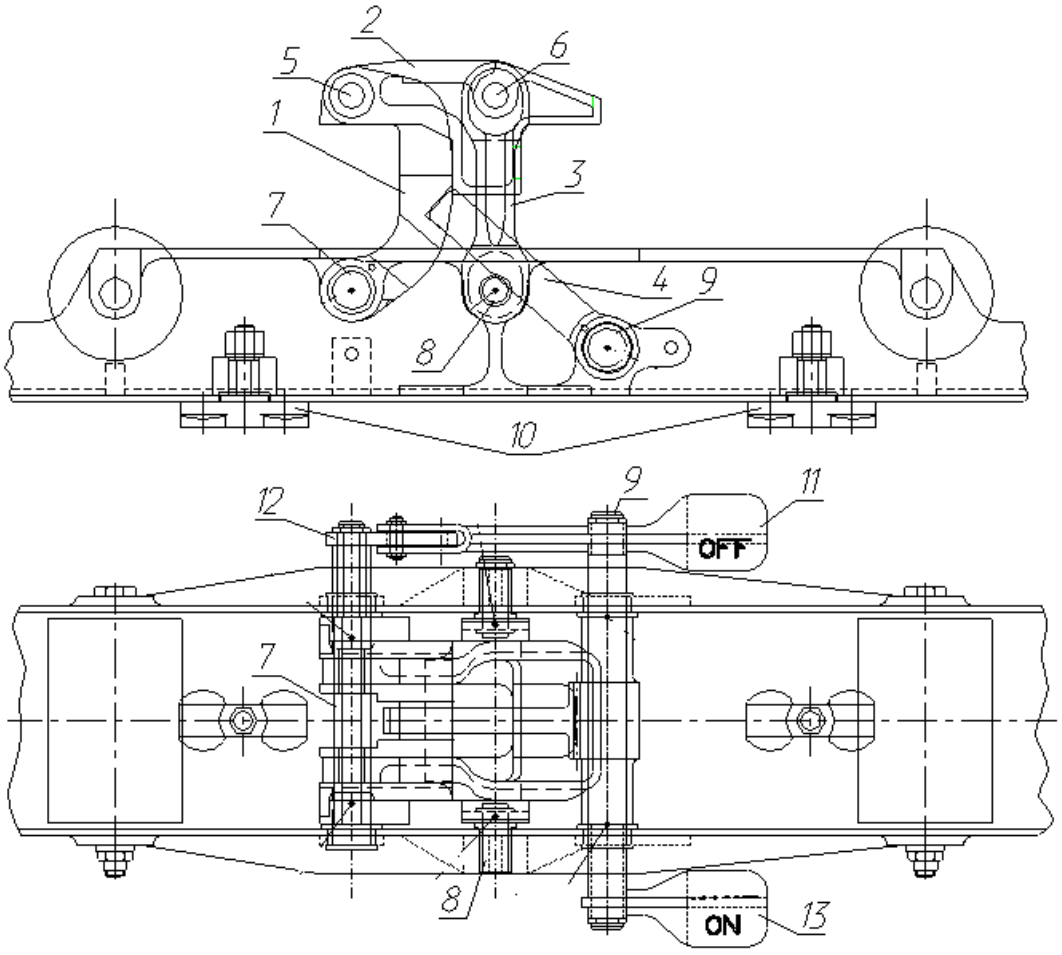

1 - Hook
2 - Capture
3 - Earring
4 - Stop
5,6 - Roller
7,8,9 - Axis
10 - Knot
11, 13 - Pedal
12 – Leash

Figure 4.1 - Construction of the XZ latch with pedal

4.2 Strength calculation of the XZ latch with pedal

The finite element model of the XZ latch with pedal has been created. The calculation was made in the NX NASTRAN program. Loads were applied to the finite element model, and fastening was modeled, material properties were set.

Using this model, the loads acting at the points of fastening of the XZ latch with pedal in the profile of the roller track are determined.

Consider three possible options for the perception of vertical load:

1) when installing the rear cargo in flight relative to the XZ latch;

2) when installing the forward cargo on the flight relative to the XZ latch;

3) when installing 2 cargo at the same time.

The load is applied using an absolutely rigid body with a contact surface. The body is restrained in all directions, except for the one in which the load acts.

1) Installation of the rear cargo in flight relative to the XZ latch:

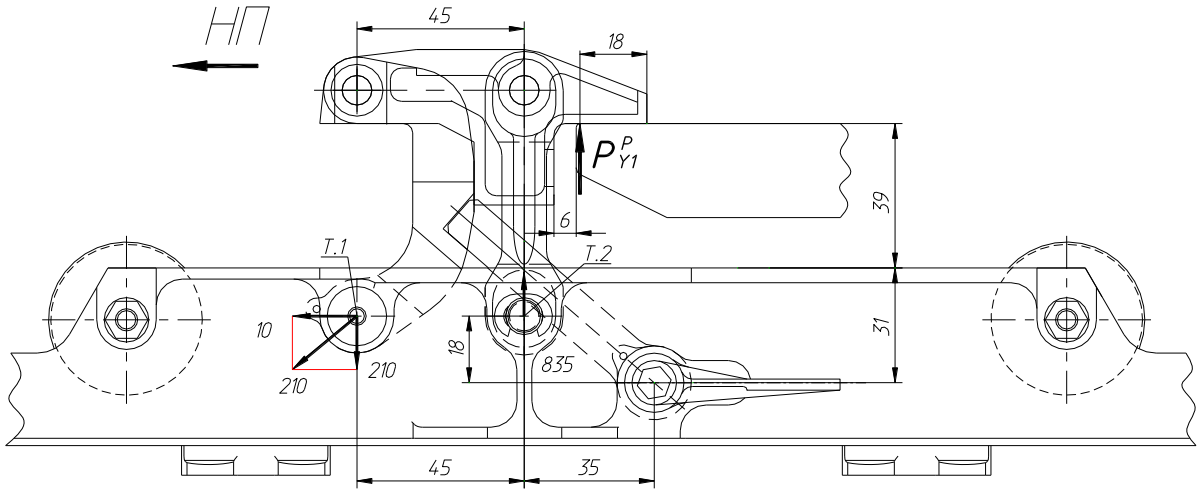

Figure 4.2 - Scheme 1

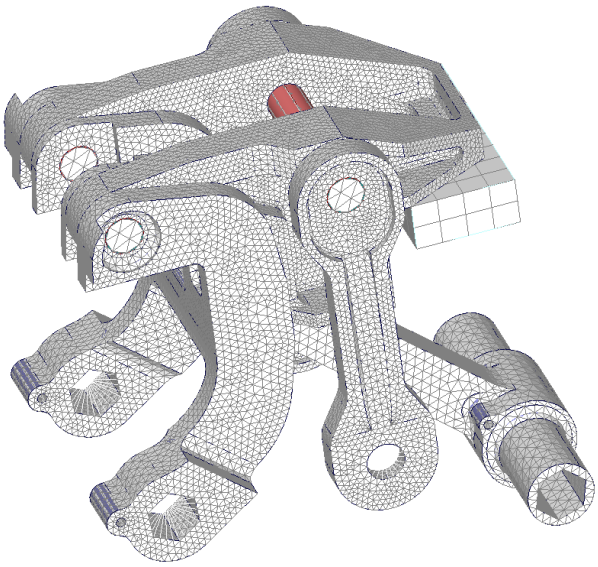

Figure 4.3 - Mesh model of the XZ latch

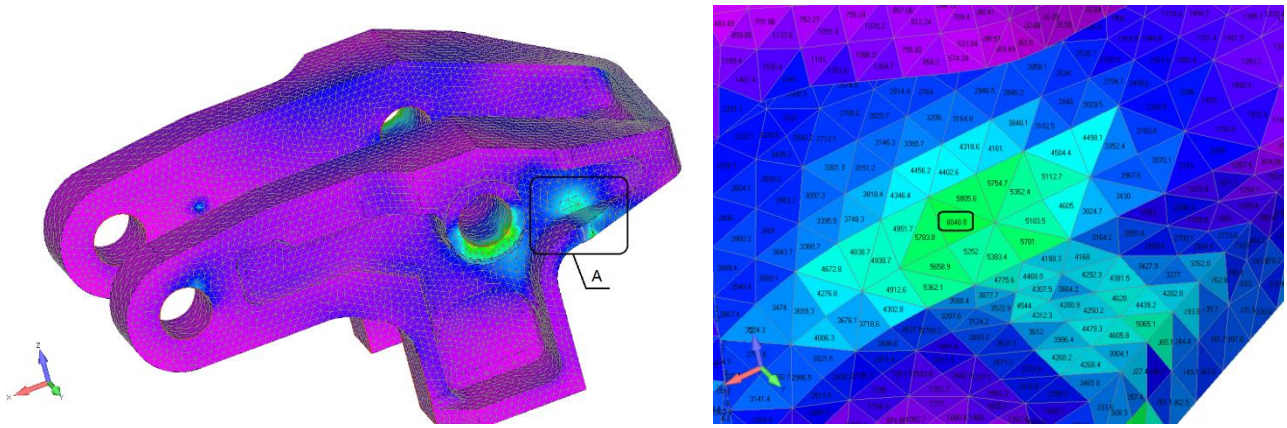

Figure 4.4 - Equivalent Stress Distribution (kgf/cm^2) in capture

Maximum equivalent stresses occurring in the capture:

$$\sigma_{eq}^{p} = 6048\,кgf/см^2.$$

2) Installation of the forward cargo on the flight relative to XZ latch:

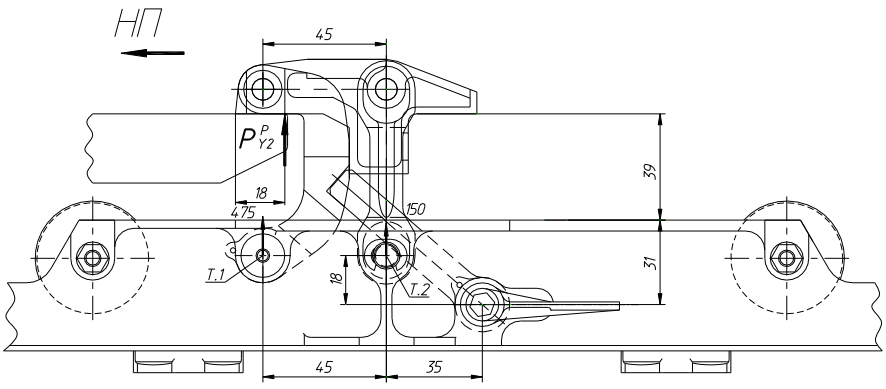

Figure 4.5 - Scheme 2

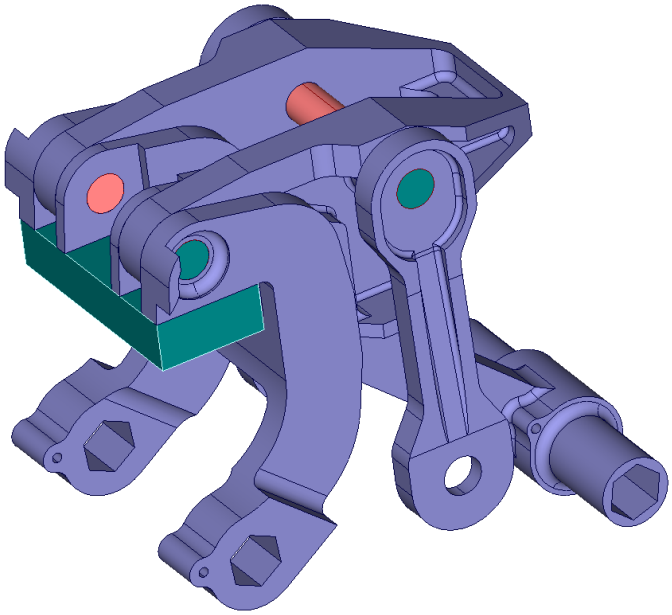

Figure 4.6 - Model of the XZ latch

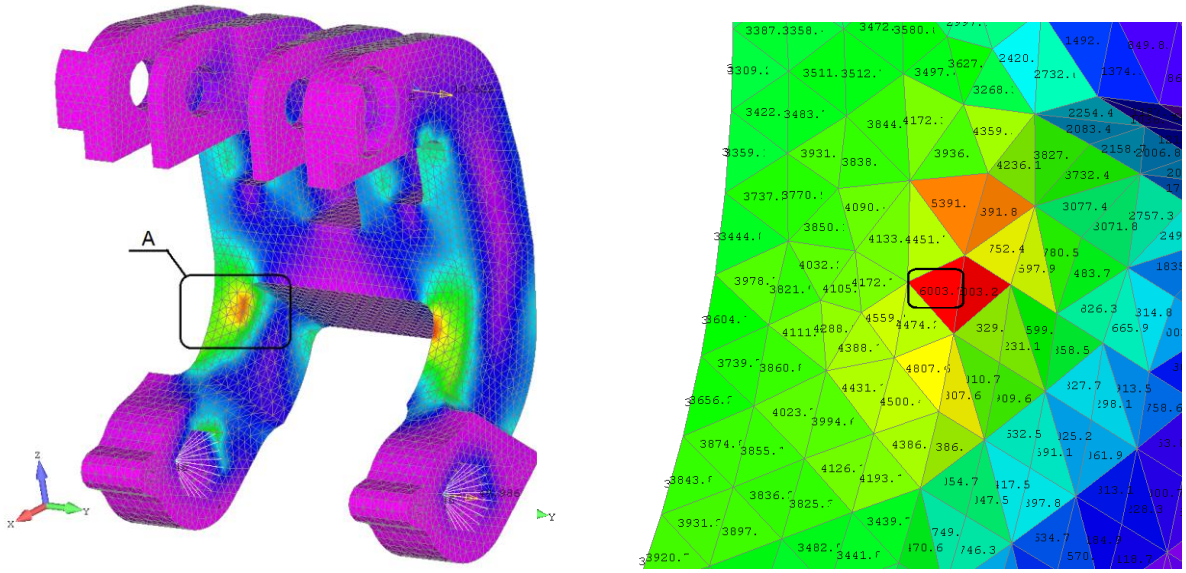

Figure 4.7 - Equivalent Stress Distribution (kgf/cm^2) in hook

Maximum equivalent stresses occurring in the hook:

$$\sigma_{eq}^{p} = 6003\ кgf/см^2.$$

3) Installation of 2 cargo at the same time:

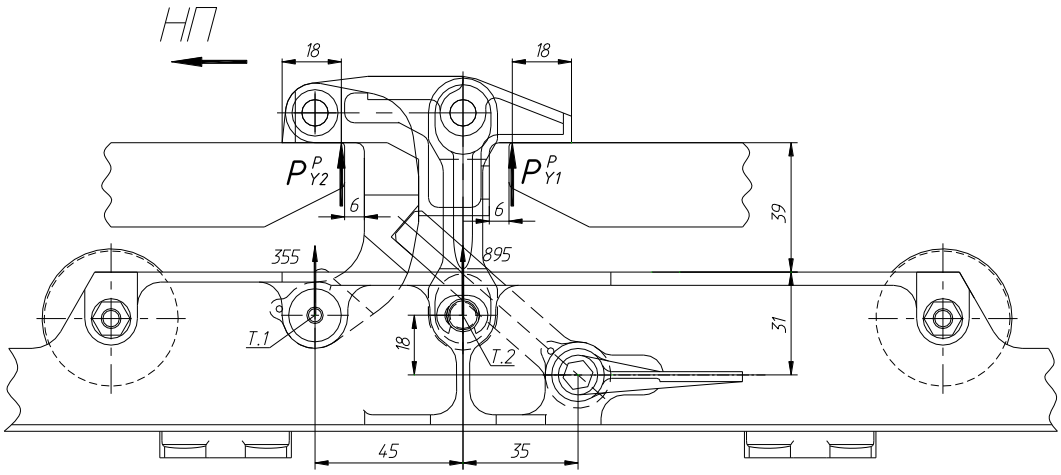

Figure 4.8 - Scheme of XZ latch with pedal

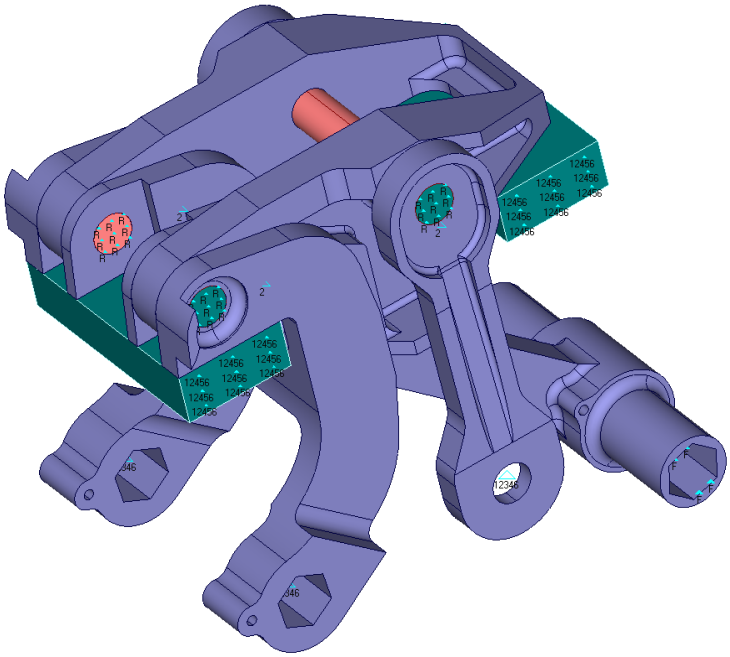

Figure 4.9 - Model of the XZ latch with pedal

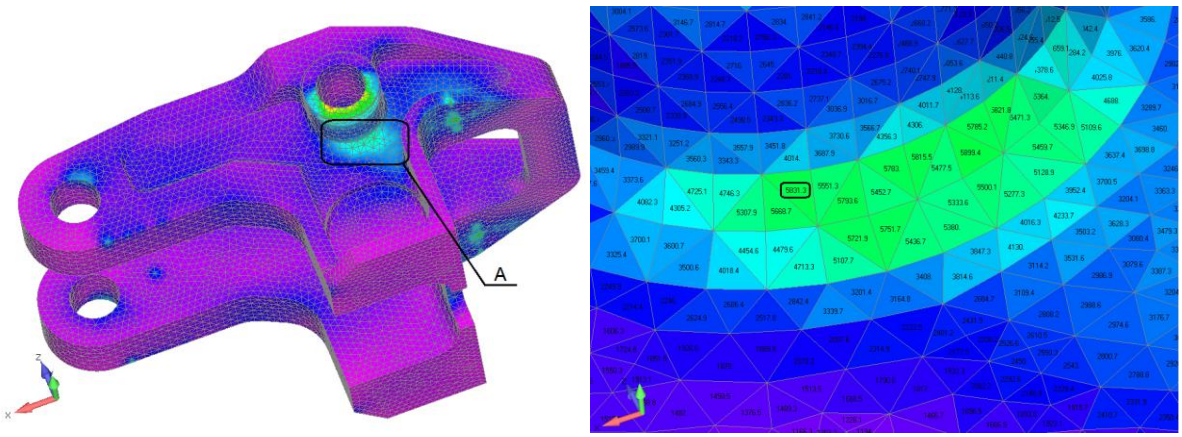

Figure 4.10 - Equivalent Stress Distribution (kgf/cm^2) in capture

Maximum equivalent stresses occurring in the capture:

$$\sigma_{eq}^{p} = 5831\ кgf/см^2.$$

4) Loading case:

Landing $\begin{cases} n_x^p = +2,05; \\ n_y^p = -3,5; \end{cases}$

Максимальная нагрузка возникает при 4-ом варианте загрузки.

$$P_X^p = 5120\ кgf;$$

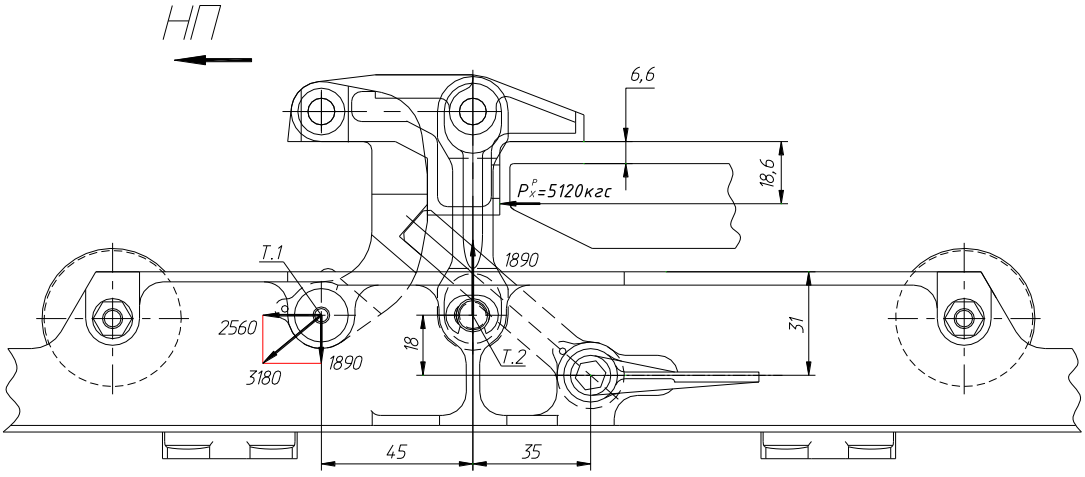

Figure 4.11 - Loading scheme of the XZ latch

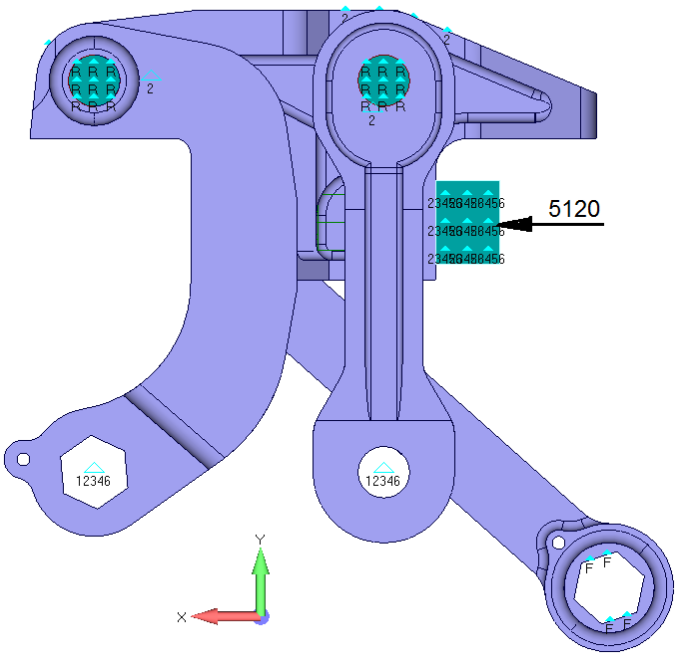

Figure 4.12 - Model of the XZ latch

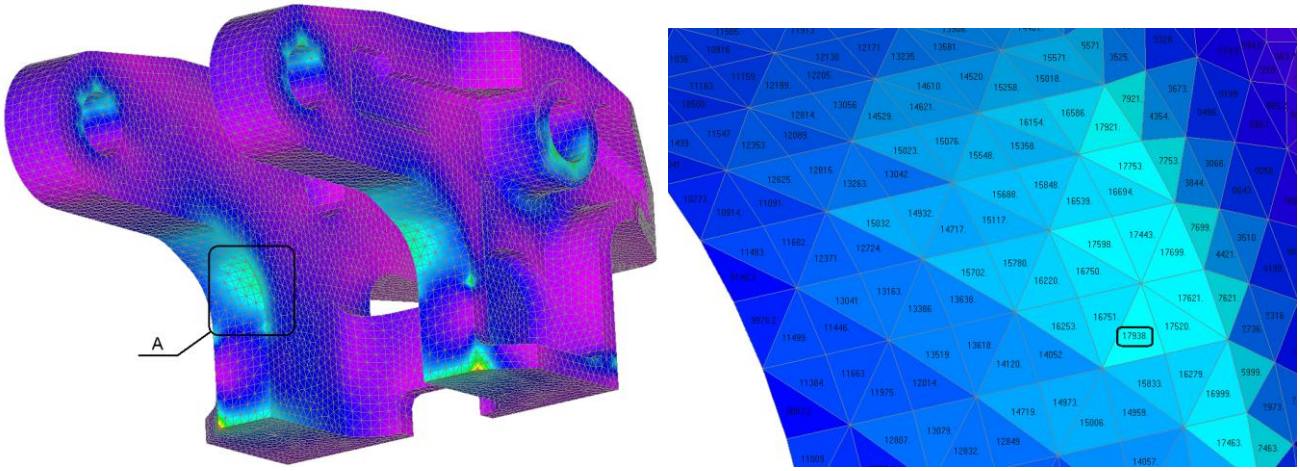

Figure 4.13 - Equivalent Stress Distribution (kgf/cm^2) in capture

Maximum equivalent stresses occurring in the capture:

$$\sigma_{eq}^{p} = 17938\,\kappa gf/cм^2.$$

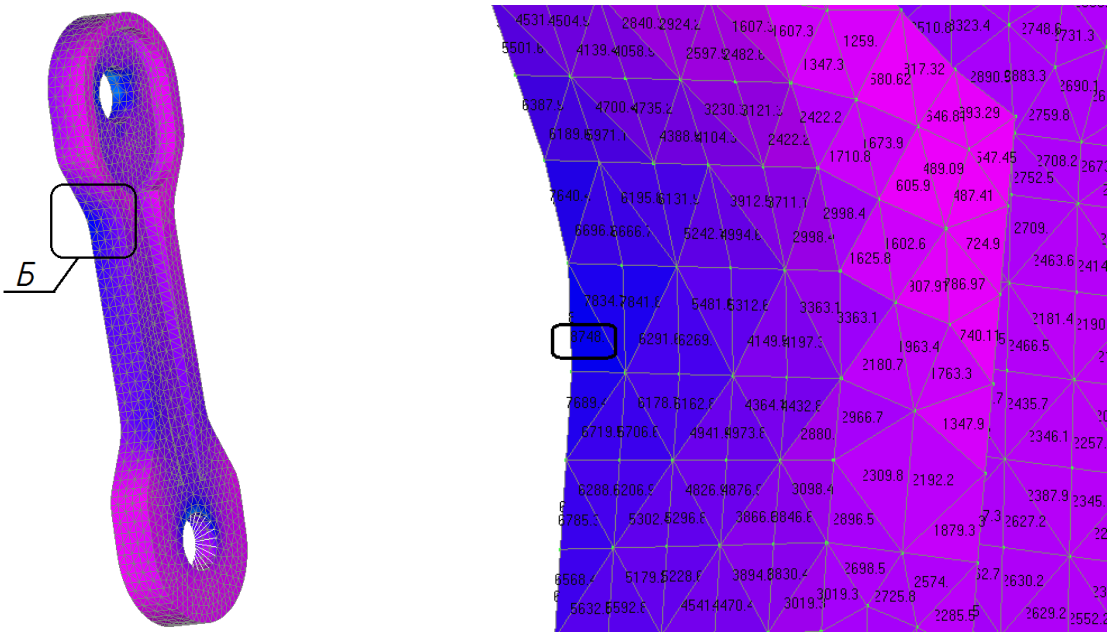

Figure 4.14 Equivalent Stress Distribution (kgf/cm^2) in earring

Maximum equivalent stresses occurring in the earing:

$$\sigma_{eq}^{p} = 8748\,кgf/см^2.$$

Loading case:

5) Take-off $\begin{cases} n_x^p = -0{,}93; \\ n_y^p = -2{,}8. \end{cases}$

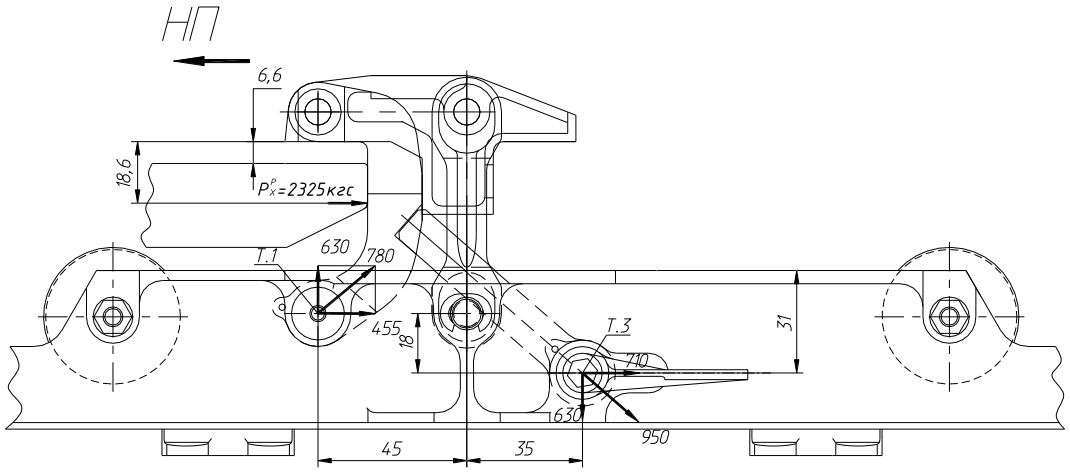

Figure 4.15 - Loading scheme of the XZ latch

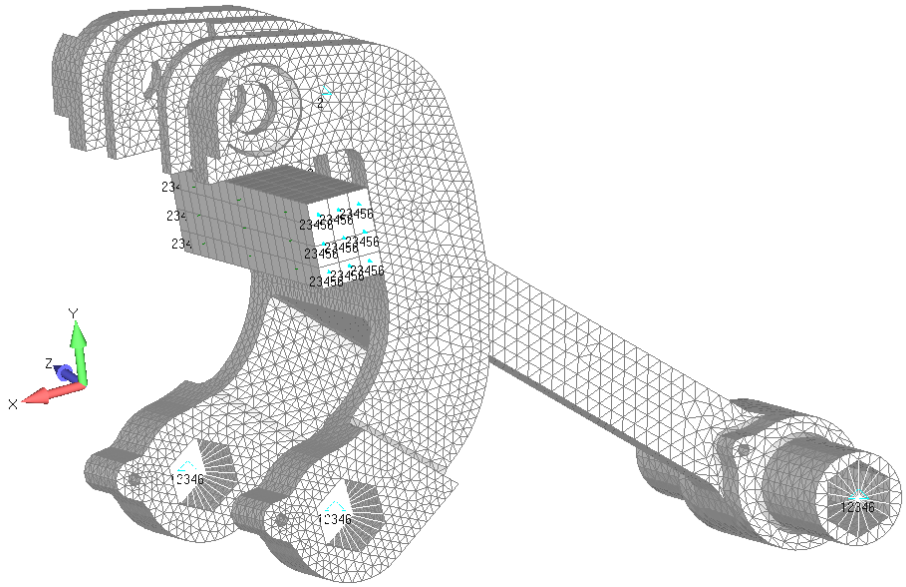

Figure 4.16 - Model of the XZ latch

The calculated loads on the attachment points of the XZ latch elements are shown in Figure 4.16.

4.3 Static test of the XZ latch

The object of testing was the XZ latch, dismantled from the roller section No. 4.

Purpose of tests. The purpose of the test is acknowledgment of static strength of the mechanical lock from the " Roller section tracks on the cargo floor ".

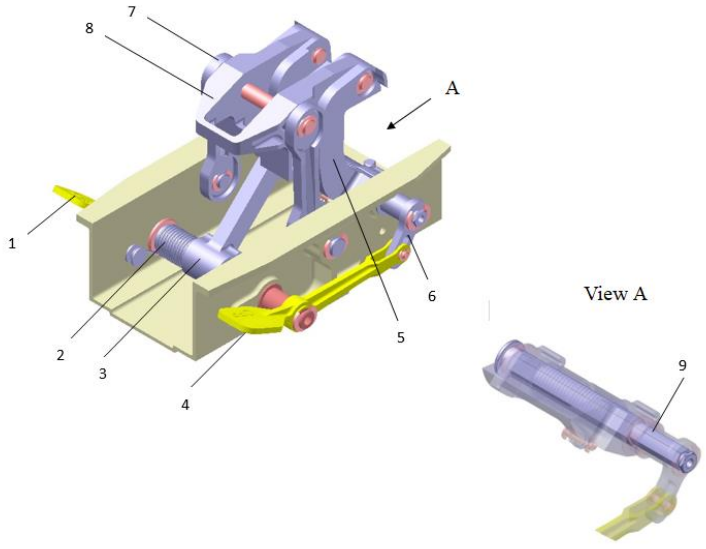

Figure 4.17 - General view of XZ latch construction

To carry out static tests of the XZ latch, a stand was manufactured and mounted. The XZ latch in the stand was installed in the open position and using a device. The loading was done according to the requirements and tasks with the help of device 1. The loading diagram of the XZ latch is shown on the Figure 4.18. Loading of the XZ latch was carried out with the help of hydrocylinder connected to the manual pump. Control of the applied loading was carried out with tanzometric strain sensor with the secondary device KCT-4 with an error less than 1%. The general view of the stand is shown on Figure 4.17.

The tests were carried out in the following sequence.

Tests up to 100% $P^{P.}$

To the XZ latch, set in the stand in the open position, with the tool 1 was applied load $P^{P}_{x} = 5120$ kgf . The load was applied in steps 20% of P^{P} to 100 % P^{P}. After removal of the load to 0 was executed inspection of construction of the XZ latch- residual deformations, cracks and other damages are not detected, also was performed checking of the latch for closing and opening- observations were not revealed.

Tests before destruction.

To the XZ latch was applied load until destruction. The load was applied in steps of 20% of the P^{P}. When the load reached 110% P^{P} (110% $P^{P}_{x} = 5632$ kgf), a click was heard. The tests were stopped. After removing the load to 0 and visual inspection of the XZ latch was detected, that the axis was destroyed.

(see Figure 4.21). Destruction of other structural elements of the XZ latch was not detected.

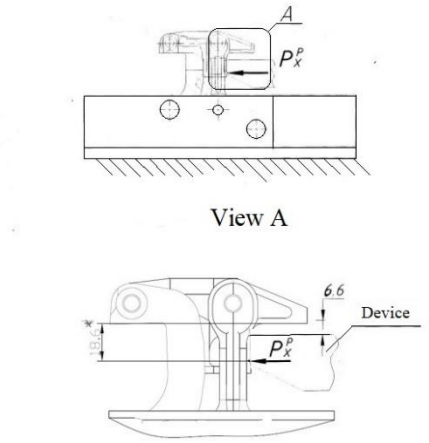

Figure 4.18 - Loading scheme of the XZ latch

Figure 4.19 - General view of the XZ latch test stand

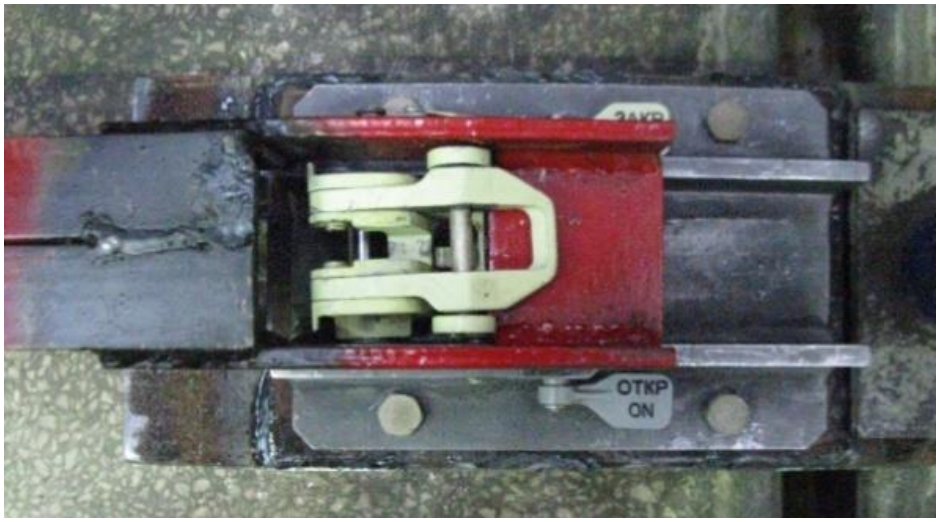

Figure 4.20 – View A

Figure 4.21 - General view of the axis destroyed during static tests of the XZ latch

Conclusion to part 4

New design for the roller equipment XZ latch has been proposed, analysed, and tested.

Stress-Strain analysys has been carried out by the Finite Elements method with assessment of the equivalent stresses according to the Mises criterium for multiaxial loading.

Equivalent stresses calculation of the main parts was provided in the NX NASTRAN program. The results of the tests carried out indicate that the static strength of the XZ latch, from the roller section on the cargo floor is 110% P^{R}_{x} (110% P^{R}_{x} = 5632 kgf).

5 LABOR PROTECTION

5.1 Analysis of harmful and dangerous production factors

CNC miller workplace is part of the production area in 100 m^2 for three workplaces, equipped with artificial lighting above each of them in addition to lamps above the machine and on the desktop, ventilation and air conditioning system. It is also equipped with technical equipment and devices such as: milling machine with CNC, closet with the tools and accessories to the machine. The top of the cabinet is intended for technological documentation. The call of the master or mechanic is carried out from the console. To the left of the worker is a container with processed or intended for milling workpieces. Chips put in a box. Equipment are placed in the cabinet.

The rational organization of the workplace provides a system of measures to ensure the optimal location of equipment and devices, the maximum use of their technical capabilities, uninterrupted provision of everything necessary for the operation, and cleanliness. With proper organization of the workplace, the milling machine operator does not need to spend time looking for devices, blanks and tools, clarifying technological documentation.

Worker use such equipment:

- finger mills with a diameter of 4 to 10 mm;
- collets;
- bushings of different sizes;
- cones;
- tapered mandrels;
- clamping bolts for cutters;
- adjusting rings;
- clamping bolts;
- clamping strips;
- different linings;
- spanners;
- vice wrench;

- key for three-jaw chuck;
- scribe;
- kern;
- file;
- vernier caliper;
- ruler;
- square;
- screwdriver;
- dural hammer;
- oiler;
- cleaning materials;
- brush;
- chip scoop.

According to the standard ГОСТ 12.0.003-2015 some harmful and dangerous factors can impact the worker [13].

Physical hazardous and harmful production factors are:

Moving parts of production equipment; moving products, blanks, materials; crumbling structures.

This factor can occur in case of injury of worker's body by piece, pull out of attachment when handling. Depart parts when milling is always associated with improper its fastening, or to a defect or deterioration of the respective devices.

Increased temperature of surfaces of equipment, materials;

On metal cutting machines, a voltage of up to 380 V is usually used. An electric burn is a consequence of heating parts of the human body when an electric current pass through them. Machine operators develop reddening of the skin.

Chemical dangerous and harmful production factor is:

Penetration into the human body through respiratory organs.

During milling, the air in the working area can be contaminated with dust from the material being processed, as well as coolant fumes. This can result in irritation of the respiratory tract.

Psychophysiological dangerous and harmful production factor by the nature of the action is:

Static overload due to monotony of work.

Milling of metals with a deviation from labor protection standards leads to exposure of hazardous production factors on workers and the most harmful is chemical factor, which can affect respiratory organs with coolant fumes.

5.2 Measures to reduce the impact of harmful and dangerous production factors

The main task of ventilation is to remove polluted or heated air from the room and supply fresh air that meets regulatory requirements, as well as to exclude the possibility of harmful substances in the air that exceed the maximum permissible concentration (MPC).

General ventilation is designed to assimilate excess heat, moisture and harmful substances in the entire volume of the working area of the room.

The calculation of the amount of supply air required for general ventilation is performed on the basis of the release of harmful substances (for example, CO) in the production area and excess sensible heat [14]. The calculation of air exchange is made in accordance with the requirements of СНиП 2.04.05-91 “Heating, ventilation and air conditioning. Design standards ".

The total amount of air L (air exchange) that must supplied by general ventilation to the production room for ensuring in the working area the maximum permissible concentration of harmful gases, vapors and dust, calculated by the formula:

$$L = \frac{M}{k*(C_{mpc}-C_{0)}} m^3/h \qquad (5.1)$$

where:

L- is the amount of supply or exhaust air depending on the adopted scheme of mechanical ventilation, m/h,

M – intensity emission of the considered harmful substance in the room, mg/h;

k - dimensionless coefficient of uniformity of distribution

ventilation air in the room;

C_{mpc} - maximum permissible concentration of harmful substances in room, mg / m. Determined from GOST 12.1.005-88 "General sanitary and hygienic requirements for the air in the working area";

C_0 -is the concentration of harmful substances in the outdoor air supplied to

room, mg/m^3.

Calculate the air exchange required to dilute toxic substances when mineral oils enter the room air in an amount of 100 mg / hour. According to GOST 12.1.005-2015, C_{npc} = 5 mg/m^3. Concentration of a toxic substance in the supply air of a room C_0 = 0.5 mg/m. Thus, the amount of air required to dilute toxic substances with a uniform distribution of harmful substances in the room (k= 1) will be:

$$L = \frac{100}{1*(5-0,5)} = 22,2\ m^3/h \quad (5.2)$$

The total cross-sectional area of the ventilation ducts is calculated:

$$\Sigma F = \frac{L}{15\ 948\psi\sqrt{\frac{h(\rho_o-\rho_i)}{\rho_o}}}\ m^2 \quad (5.3)$$

where:

ψ- coefficient, taking into account the resistance to air movement in the ducts;

h- exhaust duct height, m;

ρ_o- outside air density, kg/m^3;

ρ_i- indoor air density, kg/m^3.

Air density:

$$\rho = \frac{353}{273+t}\ kg/m^3 \quad (5.4)$$

where:

t- air temperature at which density is determined, C °.

Outside air density:

$$\rho_o = \frac{353}{273+10} = 1{,}247\ kg/m^3 \quad (5.5)$$

Indoor air density:

$$\rho_i = \frac{353}{273+23} = 1{,}192\ kg/m^3 \quad (5.6)$$

Then, the total cross-sectional area of the ventilation ducts:

$$\Sigma F = \frac{22{,}2}{15\,948*0{,}5\sqrt{\frac{3{,}5(1{,}247-1{,}192)}{1{,}247}}} = 0{,}007\ m^2 \quad (5.7)$$

The cross-sectional area of one exhaust shaft is taken constructively, taking into account the normalized range of deflector sizes. Calculate the number of channels:

$$n_{ex} = \frac{\Sigma F}{f} = \frac{0{,}007}{0{,}3} = 0{,}03 \quad (5.8)$$

Exhaust air volume through one deflector:

$$L_d = \frac{L}{n_{ex}} = \frac{22{,}2}{0{,}03} = 740\ m^3/h \quad (5.9)$$

Deflector pipe diameter:

$$D_p = 0{,}0188\sqrt{\frac{L_d}{k_{ef}\upsilon_w}} = 0{,}0188\sqrt{\frac{740}{0{,}4*4}} = 0{,}404\ m \quad (5.10)$$

where:

k_{ef} - the efficiency factor;

υ_a - is the average wind speed.

5.3 Labor Safety Instruction

1.1. Persons at least 18 years old, who have completed professional training and have a certificate for the work on CNC machines, have been trained in safe working practices, have been instructed in labor protection and fire safety are allowed to work on CNC milling machines.

1.2. The results of the briefing are recorded in the register of briefings at the workplace with a sign of the instructed and instructing person and the date of the briefing.

1.3. The frequency of re-briefing is at least once every three months.

1.4. Persons working on CNC milling machines are required perform work by which they are instructed.

1.5. Use tools and attachments only for their intended purpose.

1.6. Do not go to work on another machine, do not allow other persons to work on your machine without the permission of the master.

1.7. Workers are provided with overalls, safety footwear and other personal protective equipment in accordance with the current regulations.

1.8. Operating CNC milling machines are dangerous when removing chips, taking control measurements, changing sticks, etc.

1.9. The responsibility of the requirements for violations of the instructions of this worker is subject to disciplinary procedure.

2. Safety requirements before starting work.

2.1. Tidy up your clothes: fasten the cuffs of the sleeves with buttons, remove the hair under the headdress (for women, under a beret or a kerchief without hanging ends).

2.2. Lay the workpieces received for milling in such order that they do not obstruct the workplace and passages.

2.3. Inspect the machine and make sure that its control mechanisms are in good working order, in the presence of protective grounding, fencing and primary fire extinguishing equipment.

2.4. Make sure that you have a set of tools, accessories and their serviceability.

2.5. Adjustment of the CNC machine should be performed according to the appropriate manual for this type of equipment.

2.6. Study the drawing and get acquainted with the technology of the manufactured parts.

2.7. Upon detection of the fault of equipment, fixtures, tools, protective equipment, etc. immediate inform supervisor and do not start work until the elimination of fault.

3. Safety requirements during the performance of work.

3.1. The operator (worker) must know and follow the general safety rules for servicing metalworking machines.

3.2. To protect eyes from chips use protective glasses and, if necessary, hearing protection.

3.3. Change the position of the clamps, make control measurements, eliminate malfunctions, change blanks of parts only when the machine is turned off.

3.4. Do not remove chips while the machine is running.

3.5. Do not open the cabinet with electrical equipment, do not open the panels, flexible hoses that cover the current-carrying wires.

3.6. The processing of parts should be carried out with closed fences of the processing areas.

3.7. Do not use keys whose dimensions do not correspond to the dimensions of the heads of nuts and bolts.

3.8. Do not operate the machine with gloves or with bandaged fingers without rubber fingertips.

3.9. In case of deviations from the normal operation of the machine ("failures"), breakage of the tool, turn off the machine and notify the foreman.

3.10. Do not leave equipment running unattended.

3.11. You are obliged to inform the foreman about each accident that happened to you, keep the circumstances of the accident and be sure to contact the first aid post and register this accident during the day.

4. Safety requirements at the end of work.

4.1. Turn off the machine, engine, coolant, tidy up the tool and your workplace.

4.2. Clean the machine, fixture, fence from chips and dirt (cleaning the machine with compressed air is not allowed).

4.3. Lubricate the machine, hand over to the master.

4.4. Wipe clean and place the instrument in the toolbox.

4.5 Hang overalls, personal protective equipment in the locker. Do not put oiled overalls in a closed container (possible spontaneous combustion).

4.6. Notify the foreman about all malfunctions of the machine, equipment, tool.

5. Safety requirements in emergency situations.

5.1. Failure of the "zero" of the machine, press the "All stop" button; in manual mode set the tool to the starting point.

5.2. If the tool breaks while machining the part, press the "All stop" button; in manual mode move the machine spindle to the starting point, change the tool.

5.3. Maintenance of electrical equipment, repair, replacement of fuses is carried out by an electrician with the power supply disconnected and a sign posted on the switch-on panel with the inscription: "Do not turn on - people are working".

5.4. In the event of other emergencies, stop work, turn off the equipment, take people out of the danger zone, bar the access of unauthorized persons, inform the foreman. To proceed with the elimination of the consequences of the accident only after the permission of the foreman.

5.5. In the event of a fire, de-energize the equipment, inform the fire department and take measures to extinguish the fire with primary fire extinguishing means.

5.6. In case of injury, inform the administration of the workshop, inform the medical unit of the enterprise.

Conclusion to part 5

Learning problems related to safe and secure conditions in which human labor takes place is one of the most important tasks in the development of new technologies and production systems. Study and identification of working methods in industrial cases, occupational diseases, accidents, fires. Comfortable and safe working conditions are one of the main factors affecting labor safety.

6 ENVIRONMENTAL PROTECTION

6.1 Aircraft emissions

Airplanes emit huge amounts of carbon dioxide and water vapor, nitrogen oxides and soot into the atmosphere. The environmental impact of these components depends on the flight altitude.

Aircraft pollute the atmosphere due to the emission of harmful substances from the exhaust gases of aircraft engines.

Aircraft move from one airport to another during the flight, and the atmosphere is polluted on a global scale, so significant pollution occurs both in the areas of airports and on the routes of flight. Moreover, on the flight paths (at an altitude of 8-12 km) the danger of this pollution is small (flights of aircraft at high altitudes and at high speeds cause the scattering of combustion products in the upper atmosphere and large areas, which reduces their impact on living organisms), then in the airport area cannot be considered such pollution as impossible [15].

Gases in atmospheric air emit nozzles and exhaust branch pipes of engines. This process is called the emission of aircraft engines.

Gases generated by aircraft engines account near 87% of all civil aviation emissions, which also include emissions from special vehicles and stationary sources.

Unfavorable modes of operation are low speeds and "idling" of the engine, when pollutants are emitted into the atmosphere in quantities significantly exceeding the emission at load modes.

Emissions from aircraft engines affect the vital elements of the ecosystem: air quality, its temperature (and with it atmospheric circulation and climate) and the UV radiation flux reaching the Earth's surface.

The pollution of the biosphere by the combustion products of aviation fuels is the first aspect of the impact of air transport on the environmental situation, however, aviation has a number of distinctive features compared to other modes of transport:

the use of mainly gas turbine engines determines a different nature of the processes occurring in them and the structure of exhaust gas emissions;

the use of kerosene as a fuel leads to a change in the components of pollutants;

aircraft flights at high altitudes and at high speeds lead to the dispersion of combustion products in the upper atmosphere and over large areas, which reduces the degree of their influence on living organisms.

Exhaust gases from aircraft engines account for 75% of all civil aviation emissions.

The chemical composition of emissions from fuel combustion largely depends on the type and quality of fuel, production technology, the method of combustion in the engine and the technical condition of the engine technical condition [16].

The main components of exhaust gases of modern aircraft engines that pollute the atmosphere:

- sulfur oxides SOx;
- nitrogen oxides NOx;
- carbon monoxide CO;
- hydrocarbons that are not completely burned;
- aldehydes;
- soot (fine particles of pure carbon) - is released in the form of a train behind the engine nozzles during the takeoff of the aircraft (soot is generally released a little).

In the off-road area during the take-off of the aircraft, approximately 50% of emissions in the form of microparticles, including many heavy metals, are immediately dispersed in the areas adjacent to the airport. The rest is in the air for several hours in the form of aerosols, and then also settles on the ground. The concentration of harmful components of the exhaust gases of aircraft engines in the air and the speed of their propagation throughout the airport largely depends on the meteorological conditions. In this case, the influence of the direction and speed of the wind is most clearly traced. Other factors - air temperature and humidity, solar radiation - although they affect the concentration of pollutants, but this influence is less pronounced and has a more complex relationship.

In order to create a unified approach to the standardization of pollutant emissions, ICAO introduced the concept of a standard take-off and landing cycle, which includes all

aircraft operations from engine start to 1000 m, as well as from landing from 1000 m to engine stop. after landing the plane.

6.2 Calculation of the emissions

Emissions of CO and NO_x at the airport zone are calculated for takeoff and landing cycle. Characteristics of regimes and their duration are given in Table 6.1.

Table 6.1 - The typical takeoff and landing cycle of aircraft engine power conditions

Number of regime	Characteristics of regimes	Relative thrust $\overline{R}$	Duration of regime t, min
1	Start, idle running before takeoff (regime of low gas)	0,07	15,0
2	Takeoff	1,0	0,7
3	Climb	0,85	2,2
4	Approach landing from a height of 1000 m	0,3	4,0
5	From landing taxiing (regime of low gas)	0,07	7,0

Table 6.2 - Emission indexes of CO and NO_x during ground operations with different aircraft engine types (kg of detrimental compound / kg of fuel)

Type of aircraft	Maximal thrust of engine R_0, kN	Type of aircraft engine	Quantity of engines n	$C_{SP\,LG}$, kg/N·hour	Emission index k	
					CO	NO_2
Short-range	63,76	Turboprop D-36	2	0,049	0,0546	0,0054

Table 6.3 - Weight rate of CO and NO_x emissions by different aircraft type

Type of aircraft	Annual quantity of flights N	Relative thrust $\overline{R}$ of regimes 2, 3, 4 relatively	Weight rate of emissions W, kg/hour	
			CO	NO_2
Short-range	125	1 0,85 0,3	6,0 7,5 18,0	89 61 11

Calculations of annual emissions of CO and NO_x from aircraft engine are based on formulas:

$$M_{CO} = M_{CO\,GO} + M_{CO}\,T_{LO}$$

$$M_{NOx} = M_{NOxGO} + M_{NOx}\,T_{LO}$$

Where, $M_{CO\,GO}$, $M_{NOx\,GO}$ - masses of CO and NO_x, which are emitted during ground operations (start, idle running, from landing taxiing – regimes 1, 5);

$M_{CO\,TLO}$, $M_{NOx\,TLO}$ - masses of CO and NO_x respectively, which are emitted during takeoff and landing operations (takeoff, climb to 1000 m, approach landing from a height of 1000 m – regimes 2, 3, 4).

$$M_{CO\,GO} = K_{CO} \cdot C_{SP\,LG} \cdot R_{LG} \cdot T_{LG}$$

$$M_{NOxGO} = K_{NOx} \cdot C_{SP\,LG} \cdot R_{LG} \cdot T_{LG}$$

Where, K_{CO}, K_{NOx} – emission indexes (kg of detrimental compound per kg of fuel) of CO and NO_x relatively during ground operations (Table 6.2);

$C_{SP\ LG}$ – specific consumption of fuel during regime of low gas, kg/N·hour (Table 6.2);

R_{LG} – engine thrust at low gas,

$$R_{LG} = \overline{R} \cdot R_0$$

Where, $\overline{R}$ – relative thrust (table 6.2), R_0 – maximal thrust of engine, N (Table 6.2);

Calculations of CO and NO_x emissions relatively during takeoff and landing operations (regimes 2, 3, 4) are based on formula:

$$M_{CO\,TLO} = W_{CO\,T} \cdot T_T + W_{CO\,C} \cdot T_C + W_{CO\,L} \cdot T_L$$

$$M_{NOx\,TLO} = W_{NOxT} \cdot T_T + W_{NoxC} \cdot T_C + W_{NoxL} \cdot T_L$$

Where, $W_{CO\ T}$, $W_{NOx\ T}$ – weight rate of CO and NO_x emissions relatively during aircraft takeoff, kg/hour (table 6.3);

$W_{CO\ C}$,$W_{NOx\ C}$ – weight rate of CO and NO_x emissions relatively during climb to 1000 m;

$W_{CO\ L}$, $W_{NOx\ L}$ – weight rate of CO and NO_x emissions relatively during Approach landing from a height of 1000 m;

T_T, T_C, T_L – operating time of engine during takeoff, climb to 1000 m and descent from 1000 m relatively (Table 6.1).

Calculations of annual emissions of CO and NO_x of aircraft at the zone of airport per year are based on formulas:

$$M_{CO\ AZ} = M_{CO} \cdot N \cdot n$$

$$M_{NOx\ AZ} = M_{NOx} \cdot N \cdot n$$

where N – annual quantity of takeoff-landing of the aircraft at the airport;

n – quantity of engines of the aircraft.

For short-range turboprop aircraft engine thrust at low gas calculated as:

$$R_{LG} = 0.07 \cdot 63{,}76 = 4463{,}2 \text{ (N)} \quad (6.1)$$

Masses of CO and NOx which are emitted during ground operations:

$$M_{CO\ GO} = 0.0546 \cdot 0.049 \cdot 4463{,}2 \cdot 0.37 = 4{,}418 \text{ (kg)} \quad (6.2)$$

$$M_{NOx\ GO} = 0.0054 \cdot 0.049 \cdot 4463{,}2 \cdot 0.37 = 0{,}43695 \text{ (kg)} \quad (6.3)$$

Masses of CO and NO_x emissions relatively during takeoff and landing operations:

$$M_{CO\ TLO} = 6 \cdot 0.017 + 7.5 \cdot 0.037 + 18 \cdot 0.067 = 1.59 \text{ (kg)} \quad (6.4)$$

$$M_{NOx\ TLO} = 89 \cdot 0.017 + 61 \cdot 0.037 + 11 \cdot 0.067 = 4.15 \text{ (kg)} \quad (6.5)$$

Determine annual emissions of CO and NOx from D-36 engine:

$$M_{CO} = 4{,}42 + 1.59 = 6{,}01 \text{ (kg)} \quad (6.6)$$

$$M_{NOx} = 0{,}44 + 4.15 = 4.59 \text{ (kg)} \quad (6.7)$$

Emissions of CO and NO_x of aircraft at the zone of airport per year:

$$M_{CO\ AZ} = 6{,}01 \cdot 125 \cdot 2 = 1502 \text{ (kg/year)} \quad (6.8)$$

$$M_{NOx\ AZ} = 4{,}59 \cdot 125 \cdot 2 = 1147 \text{ (kg/year)} \quad (6.9)$$

The ICAO standard according to control emission parameters for modern engines has standard value for relations between masses of CO and NOx and maximal thrust of engine.

For engine D-36 these relations are next:

$$M_{CO}/R_0 = 6010 / 63,76 = 94,25 \text{ (g/kN)} \quad (6.10)$$

$$M_{NOx}/R_0 = 4590 / 63,76 = 71,98 \text{ (g/kN)} \quad (6.11)$$

According to ICAO standard relation looks like:

$$M_{CO}/R_0 = 118 \text{ g/kN}, M_{NOx}/R_0 = (40...80) \text{ g/kN} \quad (6.12)$$

So, after calculations resulted values M_{CO}/R_0 and M_{NOx}/R_0 are in the allowable limits per control emission parameters for modern engines.

Conclusion to part 6

After calculations can be conclude that masses of CO and NO_x, which are emitted during ground operations, are equal 4,42 kg and 0,44 kg respectively. During takeoff and landing operations CO equal 1,59 kg and NO_x - 4,15 kg. After analyzing, it can be assumed that at the low gas regime maximum volume of emissions are produced. It is obvious that the emission of harmful substances (emission of an aircraft engine) depends on the mode of its operation and the duration of operation in this mode.

GENERAL CONCLUSIONS

According to the task for Master thesis the Optimization of the XZ latch design for Unit Load Devices has been performed.

This task was achieved by the conducting following objectives: analysis of the contemporary designs; selection of the appropriate methods and procedures; calculation of plane geometry for research and development results implementation; development of new XZ latch construction; determination of equivalent stresses occurring in construction in different loading variants, etc.

It was noticed that restrained system has quite a lot of means of different designs.

Preliminary design has been performed for investigation of the developed latch.

To prove reliability of presented design, static test and the strength calculation in NX Nastran program was provided.

The Diploma work comprises also analysis of harmful production factors during manufacturing of such latch on the CNC machine and aircraft emissions calculation.

The presented research and development is performed on the base of the concepts proposed by the Antonov Design Buero and adopted to the plane preliminary design, conducted in the frame oof the Diploma work.

REFERENCES

1. Lectures synopsis on “Equipment for Cargo and Container Compartment/ M.V. Karuskevich. – NAU, 2018 – 25p.

2. Flight Operations Support and Line Assistance. [Electronic source] – Access mode: https://www.slideshare.net/FernandoNobre1/weight-and-balance (last access November 10, 2020)

3. Flying in Cargo Class: The Anatomy of an Air Freighter. [Electronic source] – Access mode: http://www.nycaviation.com/2015/02/anatomy-freighter/38093 (last access November 10, 2020)

4. Patent on Automatic pallet locking device/ Ernest Prete, Jr., Woodland Hills – US3810534A. Ancra International LLC; Filed: Apr. 22, 1970.

5. Методичні рекомендації до виконання курсового проекту для студентів напряму підготовки 6.051101 «Авіа- та ракетобудування» / [С.Р. Ігнатович та ін.] – Київ: НАУ, 2014 – 53 с.

6. NX (система автоматизированного проектирования). [Electronic source] – Access mode: https://b2b.partcommunity.com/community/knowledge/ru/detail/397/Siemens+NX(last access November 14, 2020)

7. Accelerate innovation with leading-edge 3D product design software. [Electronic source] – Access mode: https://www.plm.automation.siemens.com/global/ru/products/mechanical-design/product-modeling.html (last access November 14, 2020)

8. Метод конечных элементов в механике деформируемого твёрдого тела. Учебное пособие. / В.Г. Фокин – Самара: Изд-во Самарский государственный технический университет, 2010. – 6 с.

9. FEMAP™. [Electronic source] – Access mode: https://ideal-plm.ru/page/products_femap (last access November 14, 2020)

10. Руководство по летной эксплуатации самолета АН-74ТК-100. Книга 1. – 1991г. – 9 с.

11. Руководство по летной эксплуатации самолета АН-74. Книга 1. -1991г. – 55 с.

12. Руководство по летной эксплуатации самолета АН-74. Книга 2. -1991г. – 176 с.

13. ГОСТ 12.0.003-2015 ГОСТ. Система стандартов безопасности труда (ССБТ). Опасные и вредные производственные факторы. Классификация. Введ. 2017-03-01

14. Охрана труда. Практикум. – Минск. 2018 – 44 с.

15. Какие экологические проблемы существуют в авиации? [Electronic source] – Access mode: URL: http://olymp.as-club.ru/publ/arkhiv_rabot/pjatnadcataja_olimpiada_2017_18_uch_god/istoriko_issledovatelskaja_rabota/38-1-0-2222 (last access November 12, 2020)

16. Вплив повітряних джерел авіаційного транспорту на навколишнє природне середовище. [Electronic source] – Access mode: https://pidru4niki.com/92957/ekologiya/vpliv_povitryanih_dzherel_aviatsiynogo_transportu_navkolishnye_prirodne_seredovische (last access on November 29, 2020)

Appendix A

П Р О Е К Т
С А М О Л Е Т А С Т Р Д Д
Н А У, А К И

ПРОЕКТ Master thesis Расчет выполнен 21.09.2020
Исполнитель Dakhovnik A.S. Руководитель Karuskevych M.V.

ИСХОДНЫЕ ДАННЫЕ И ВЫБРАННЫЕ ПАРАМЕТРЫ

Количество пассажиров	0.
Количество членов экипажа	4.
Количество бортпроводников или сопровождающих	1.
Масса снаряжения и служебного груза	874.26 кг.
Масса коммерческой нагрузки	10000.00 кг.
Крейсерская скорость полета	600. км/ч
Число "М" полета при крейсерской скорости	0.5420
Расчетная высота начала реализации полетов с крейсерской экономической скоростью	8.30 км
Дальность полета с максимальной коммерческой нагрузкой	1350. км.
Длина летной полосы аэродрома базирования	1.90 км.
Количество двигателей	2.
Оценка по статистике тяговооруженности в н/кг	3.3000
Степень повышения давления	24.00
Принятая степень двухконтурности двигателя	4.00
Оптимальная степень двухконтурности двигателя	8.00
Относительная масса топлива по статистике	0.2000
Удлинение крыла	10.34
Сужение крыла	3.00
Средняя относительная толщина крыла	0.120
Стреловидность крыла по 0.25 хорд	17.0 град.
Степень механизированности крыла	1.350
Относительная площадь прикорневых наплывов	0.050
Профиль крыла – Ламинизирваный типа NACA	
Шайбы УИТКОМБА - не применяются	
Спойлеры - установлены	
Диаметр фюзеляжа	3.14 м.
Удлинение фюзеляжа	9.10
Стреловидность горизонтального оперения	25.0 град.
Стреловидность вертикального оперения	26.0 град.

Р Е З У Л Ь Т А Т Ы Р А С Ч Е Т А
Н А У, А К И, КАФЕДРА "К Л А"

Значение оптимального коэффициента подъемной силы в расчетной точке крейсерского режима полета Су 0.43436

Значение коэффициента Сх.инд. 0.00937

ОПРЕДЕЛЕНИЕ КОЭФФИЦИЕНТА Dм = Мкрит - Мкрейс

Число Маха крейсерское	Мкрейс	0.54203
Число Маха волнового кризиса	Мкрит	0.72696
Вычисленное значение	Dм	0.18492

Значения удельных нагрузок на крыло в кПА(по полной площади):

при взлете	3.273
в середине крейсерского участка	3.059
в начале крейсерского участка	3.180

Значение коэффициента сопротивления фюзеляжа и гондол 0.00669

Значение коэфф. профиль. сопротивления крыла и оперения 0.00938

Значение коэффициента сопротивления самолета:
в начале крейсерского режима 0.02784
в середине крейсерского режима 0.02747
Среднее значение Су при условном полете по потолкам 0.43436

Среднее крейсерское качество самолета 15.81108

Значение коэффициента Су.пос. 2.114
Значение коэффициента (при скорости сваливания) Су.пос.макс. 3.171
Значение коэффициента (при скорости сваливания) Су.взл.макс. 2.535
Значение коэффициента Су.отр. 1.850
Тяговооруженность в начале крейсерского режима 0.617
Стартовая тяговооруженность по условиям крейс. режима Ro.кр. 1.934
Стартовая тяговооруж. по условиям безопасного взлета Ro.взл. 2.190

Расчетная тяговооруженность самолета Ro 2.278

Отношение Dr = Ro.кр / Ro.взл Dr 0.883

УДЕЛЬНЫЕ РАСХОДЫ ТОПЛИВА (в кг/кН*ч):

взлетный	40.7208
крейсерский (характеристика двигателя)	54.5575
средний крейсерский при заданной дальности полета	54.9528

ОТНОСИТЕЛЬНЫЕ МАССЫ ТОПЛИВА:

аэронавигационный запас	0.03128
расходуемая масса топлива	0.11032

ЗНАЧЕНИЯ ОТНОСИТЕЛЬНЫХ МАСС ОСНОВНЫХ ГРУПП:

крыла	0.14565
горизонтального оперения	0.01939
вертикального оперения	0.02171
шасси	0.05147
силовой установки	0.07824
фюзеляжа	0.15697
оборудования и управления	0.12163
дополнительного оснащения	0.00192
служебной нагрузки	0.02102
топлива при Lрасч.	0.14160
коммерческой нагрузки	0.24044

Взлетная масса самолета "М.о" = 41591. кГ.
Потребная взлетная тяга одного двигателя 47.37 kH

Относительная масса высотного оборудования и
противообледенительной системы самолета 0.0172
Относительная масса пассажирского оборудования
(или оборудования кабин грузового самолета) 0.0010
Относительная масса декоративной обшивки и ТЗИ 0.0077
Относительная масса бытового (или грузового) оборудования 0.0146
Относительная масса управления 0.0081
Относительная масса гидросистем 0.0209

Относительная масса электрооборудования 0.0214
Относительная масса локационного оборудования 0.0059
Относительная масса навигационного оборудования 0.0089
Относительная масса радиосвязного оборудования 0.0045
Относительная масса приборного оборудования 0.0104
Относительная масса топливной системы (входит в массу "СУ") 0.0041

Дополнительное оснащение:

Относительная масса контейнерного оборудования	0.0000
Относительная масса нетипичного оборудования	0.0019

[встроенные системы диагностики и контроля параметров, дополнительное оснащение салонов и др.]

ХАРАКТЕРИСТИКИ ВЗЛЕТНОЙ ДИСТАНЦИИ

Скорость отрыва самолета	191.44 км/ч
Ускорение при разбеге	1.60 м/с*с
Длина разбега самолета	879. м.
Дистанция набора безопасной высоты	578. м.
Взлетная дистанция	1458. м.

ХАРАКТЕРИСТИКИ ВЗЛЕТНОЙ ДИСТАНЦИИ ПРОДОЛЖЕННОГО ВЗЛЕТА

Скорость принятия решения	181.87 км/ч
Среднее ускорение при продолженном взлете на мокрой ВПП	0.03 м/с*с
Длина разбега при продолженном взлете на мокрой ВПП	5700.90 м.
Взлетная дистанция продолженного взлета	6153.70 м.
Потребная длина летной полосы по условиям прерванного взлета	6387.80 м.

ХАРАКТЕРИСТИКИ ПОСАДОЧНОЙ ДИСТАНЦИИ

Максимальная посадочная масса самолета	39027. кг.
Время снижения с высоты эшелона до высоты полета по кругу	17.0 мин.
Дистанция снижения	28.40 км.
Скорость захода на посадку	186.58 км/ч.
Средняя вертикальная скорость снижения	1.60 м/с
Дистанция воздушного участка	484. м.
Посадочная скорость	171.58 км/ч.
Длина пробега	400. м.
Посадочная дистанция	885. м.
Потребная длина летной полосы (ВПП + КПБ) для основного аэродрома	1477. м.
Потребная длина летной полосы для запасного аэродрома	1256. м.

ПОКАЗАТЕЛИ ЭФФЕКТИВНОСТИ САМОЛЕТА

Отношение массы снаряженного самолета к массе коммерческой нагрузки	2.5623
Масса пустого снаряженного с-та приход. на 1 пассажира	0.00 кг/пас.
Относительная производительность по полной нагрузке	229.22 км/ч
Производительность с-та при макс. коммерч. нагрузке	5294.1 кг*км/ч
Средний часовой расход топлива	1799.249 кг/ч
Средний километровый расход топлива	3.40 кг/км
Средний расход топлива на тоннокилометр	339.858 г/(т*км)
Средний расход топлива на пассажирокилометр	0.0000 г/(пас.*км)
Ориентировочная оценка приведен. затрат на тоннокилометр	0.3244 $/(т*км)